Quaternary Science Reviews 140 (2016) 49–66

Contents lists available at ScienceDirect

Quaternary Science Reviews

journal homepage: www.elsevier.com/locate/quascirev

Using palynology to re-assess the Dead Sea laminated sediments – Indeed varves?

Lourdes López-Merino [a, *], Suzanne A.G. Leroy [a], Amram Eshel [b], Valentina Epshtein [b], Reuven Belmaker [c], Revital Bookman [c]

[a] Institute of Environment, Health and Societies, Brunel University London, UB8 3PH Uxbridge, UK
[b] The Ted Arisson Airborne Allergens Monitoring Laboratory, Tel Aviv University, Tel Aviv 69978, Israel
[c] Dr Strauss Department of Marine Geosciences, Charney School of Marine Sciences, University of Haifa, Mount Carmel, Haifa 31905, Israel

ARTICLE INFO

Article history:
Received 7 February 2016
Received in revised form
22 March 2016
Accepted 22 March 2016

Keywords:
Dead Sea
Laminated sediments
Aragonite
Air-borne pollen
Reworked pollen
Flash-flood events

ABSTRACT

Lacustrine laminated sediments are often varves representing annual rhythmic deposition. The Dead Sea high-stand laminated sections consist of mm-scale alternating detrital and authigenic aragonite laminae. Previous studies assumed these laminae were varves deposited seasonally. However, this assumption has never been robustly validated. Here we report an examination of the seasonal deposition of detrital-aragonite couplets from two well-known Late Holocene laminated sections at the Ze'elim fan-delta using palynology and grain-size distribution analyses. These analyses are complemented by the study of contemporary flash-flood samples and multivariate statistical analysis. Because transport affects the pollen preservation state, well–preserved (mostly) air-borne transported pollen was analysed separately from badly-preserved pollen and fungal spores, which are more indicative of water transport and reworking from soils. Our results indicate that (i) both detrital and aragonite laminae were deposited during the rainy season; (ii) aragonite laminae have significantly lower reworked and fungal spore concentrations than detrital and flash-flood samples; and (iii) detrital laminae are composed of recycling of local and distal sources, with coarser particles that were initially deposited in the Dead Sea watershed and later transported via run-off to the lake. This is in line with previous carbon balance studies that showed that aragonite precipitation occurs after the massive input of TCO_2 associated with run-off episodes. Consequently, at least for the Holocene Ze'elim Formation, laminated sediments cannot be considered as varves. Older Quaternary laminated sequences should be re-evaluated.

1. Introduction

Fine-laminated lacustrine sequences have commonly proven to be annually deposited. Thus, varve-based chronologies of these sequences can be obtained (e.g. Ojala and Alenius, 2005; Zolitschka et al., 2015). Large portions of the Dead Sea Basin (DSB) Late Quaternary sediments are laminated (Neev and Emery, 1967; Begin et al., 1974), i.e. the Lisan Formation (70–13 ka BP; Stein and Goldstein, 2006; Torfstein et al., 2013) and the Ze'elim Formation (<10 ka BP; Migowski et al., 2006). These laminated sections consist of mm-scale alternating detrital and authigenic aragonite laminae. Based on age-depth models and lamina counting, these laminae were assumed to be varves in most studies, i.e. rainy season-detrital *versus* summer-aragonite deposition (Neev and Emery, 1967; Begin et al., 1974; Heim et al., 1997; Migowski et al., 2004; Prasad et al., 2004; Neumann et al., 2009; Leroy et al., 2010; Neugebauer et al., 2015). However, the exact seasonal character of the Dead Sea laminae has not been confirmed in a robust manner. This is of extreme importance for the accurate use of the DSB laminated sediments as palaeoenvironmental and palaeoclimate archives. Therefore, the aim of this paper is to re-address the nature of these laminated sediments in order to aid accurate interpretations of environmental change in the region.

Dead Sea detrital laminae are composed of a mixture of regional dust inputs and local run-off erosion products from the catchment area (Belmaker et al., 2011; Haliva-Cohen et al., 2012). In numerous lakes, carbonate deposition is closely related to biological activity

* Corresponding author.
E-mail addresses: lourdes.lopez-merino@brunel.ac.uk (L. López-Merino), suzanne.leroy@brunel.ac.uk (S.A.G. Leroy), amrame@tauex.tau.ac.il (A. Eshel), epshtein@post.tau.ac.il (V. Epshtein), reuven.belmaker@mail.huji.ac.il (R. Belmaker), rbookman@univ.haifa.ac.il (R. Bookman).

http://dx.doi.org/10.1016/j.quascirev.2016.03.024

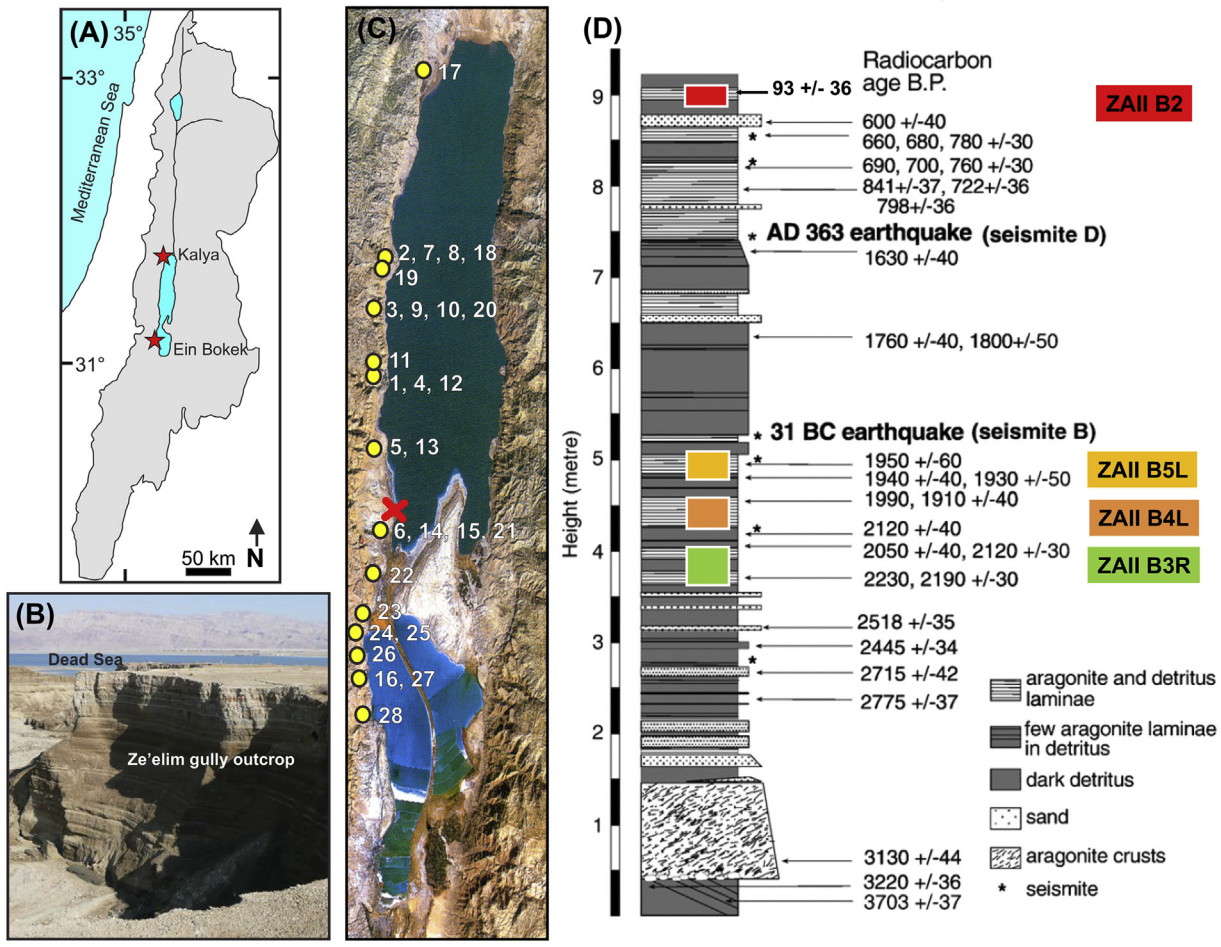

Fig. 1. (A) Location map of the Dead Sea and its watershed. Red stars indicate the location of the two aeropalynological stations. (B) Photo of the Ze'elim gully outcrop sampled in this study (Photo by L. López-Merino). (C) Location map of the laminated sediment blocks at Ze'elim and flash-flood sampling sites. Red cross indicates the location of the Ze'elim outcrop. Yellow circles indicate flash-flood sampling locations (numbers as in Supplementary Table S3 (D) Sedimentary scheme of the Ze'elim outcrop profile and radiocarbon chronology (modified from Bookman (Ken-Tor) et al., 2004). ZA11B2 sediment block represent the late 19th – early 20th centuries high-stand. ZA11B3R, ZA11B4L and ZA11B5L sediment blocks represent the Hellenistic-early Roman high-stand. Aragonite crusts were deposited in a coastal to terrestrial environment, while the aragonite laminae (discussed in this study) were deposited in a lacustrine environment. (For interpretation of the references to colour in this figure legend, the reader is referred to the web version of this article.)

(e.g. Thompson et al., 1997; Salmaso and Decet, 1998). In contrast, carbonate deposition in the Dead Sea is inorganic and results from the interaction between freshwater run-off and Dead Sea hypersaline brine (Katz and Kolodny, 1989; Stein et al., 1997). The primary origin of aragonite from the diluted upper water mass is confirmed by the excellent state of preservation of the crystals and their concentration within specific layers in the laminated sequences. This supports non-overlapping times of deposition between aragonite and detrital laminae (Heim et al., 1997; Stein et al., 1997). The commonly presumed season for aragonite precipitation is summer. The trigger is attributed to evaporation and warming of the high bicarbonate surface waters that entered via run-off during the wet season ("whitening" events) (Neev and Emery, 1967; Stein et al., 1997). On the other hand, Barkan et al. (2001) measured carbonate system parameters in the upper water mass that formed after the heavy flooding during the extreme winter of 1992 and showed that, at least in the modern Dead Sea, aragonite precipitation occurs just after the massive input of TCO_2 during the wet season. Research so far, on geochemical and palaeolimnological parameters, has not established the exact timing of the aragonite deposition and its relation to detrital input events.

Based on the observations of Barkan et al. (2001), we hypothesise that aragonite may have not been deposited during summer as is commonly interpreted, but instead the detrital-aragonite couplets may represent flash-flood events rather than an annual cycle. Thus, laminated sequences could be formed by flash-flood events delivering sediments into the lake followed by aragonite deposition in a climate-controlled lacustrine environment, i.e. precipitation in the drainage basin. To examine this hypothesis we performed grain-size and palynological analyses of detrital-aragonite couplets from two well-dated high-stand laminated sequences in the Ze'elim Formation: the Hellenistic-early Roman and the late 19th – early 20th centuries (Bookman (Ken-Tor) et al., 2004). Grain-size distribution provides information on sediment source (i.e. dust or watershed erosion), while palynology provides information on both seasonality (well-preserved, air-borne pollen) and sediment transport (reworked, water-borne pollen). In addition, palynological analysis was carried out on fine mud deposits collected immediately after modern flash-flood events, assuming that these deposits represent flood suspended matter.

2. Materials and methods

2.1. Study area and selected laminated sediments

The Dead Sea (Fig. 1A) is a closed, inland hypersaline lake (e.g.

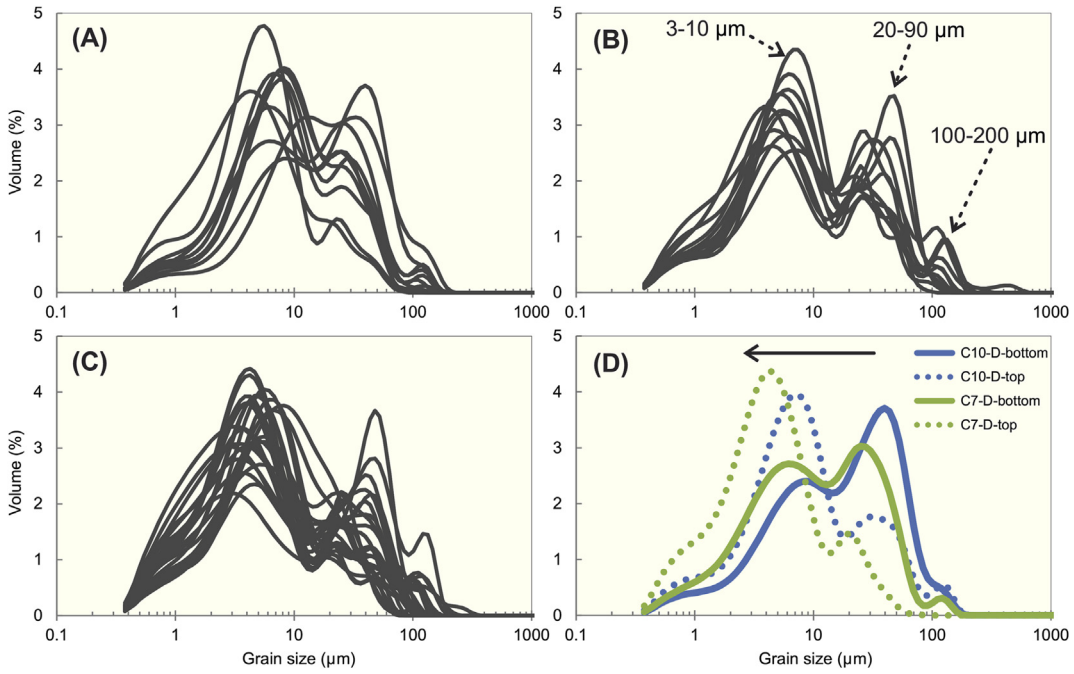

Fig. 2. Grain-size distribution in detrital samples from blocks ZA11B2 (A), ZA11B3R (B) and ZA11B5L (C). Grain-size distribution of detrital laminae C7 and C10 (numbers as in Supplementary Table S2) from block ZA11B2 showing upward fining pointing to graded bedding during flash-flood events are also shown (D).

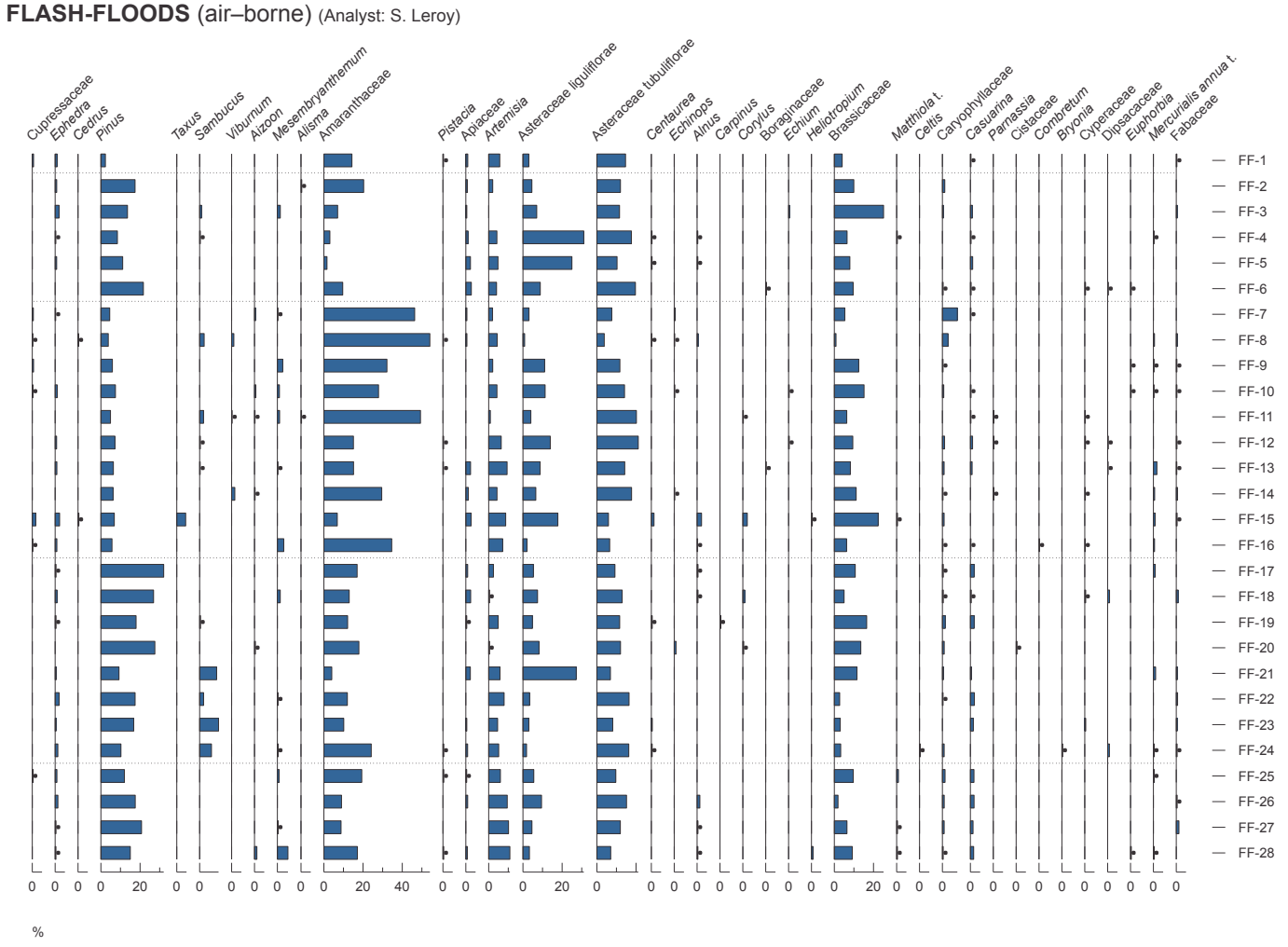

Fig. 3. Percentage diagram of well-preserved pollen (air-borne) in modern flash-flood samples. Black dots represent percentages below 0.5%. Flash-flood samples are grouped by months and ordered from North to South. Details on flash-flood samples are given in Supplementary Table S3.

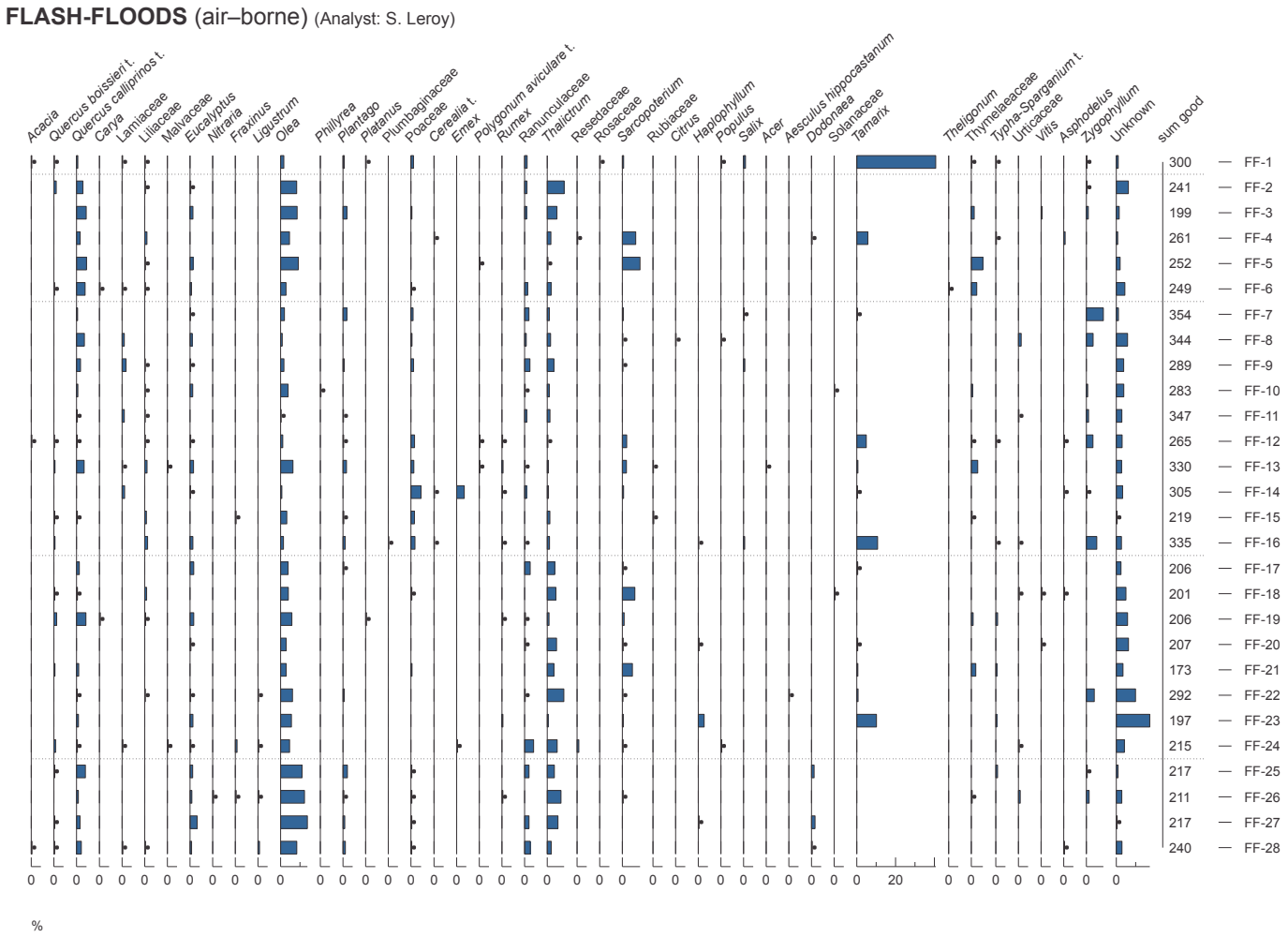

Fig. 3. (*continued*).

Niemi and Ben-Avraham, 1997) and the descendant of the larger Late Pleistocene Lake Lisan (e.g. Bookman et al., 2006; Stein, 2014). Its main fresh water tributaries are the Jordan River and flash-floods that flow west from the Jordanian Mountains and east from the Judean Mountains. Long-term fluctuations of the Dead Sea lake level are caused by rainfall fluctuations over the watershed (Enzel et al., 2003; Bookman (Ken-Tor) et al., 2004). Rain occurs between autumn and spring and it can be either spatially localised or widespread (Dayan and Sharon, 1980). The main synoptic conditions triggering rain and dust transport to the Dead Sea area are the east Mediterranean cyclones and the Red Sea trough. The former is responsible of most winter rain and dust transport, while the latter is more related to autumn and spring dust storms (Ganor and Foner, 1996; Dayan et al., 2007). Because the Dead Sea is located on the border between semiarid and arid climates, rainfall varies seasonally and annually and is often concentrated in intense showers that cause flash-flood events and erosion (Dayan and Morin, 2006; Greenbaum et al., 2006).

The Ze'elim Formation consists of the lacustrine Holocene deposits in the DSB (Fig. 1B). Extensive outcrops of the formation were described at the Ze'elim Plain, one of the largest fan deltas along the western margin of the Dead Sea (Fig. 1C). Outcrops of the Ze'elim Formation were used for palaeoclimate and palaeoseismicity reconstructions (Ken-Tor et al., 2001a, 2001b; Bookman (Ken-Tor) et al., 2004; Kagan et al., 2011). The reconstructed lake-level curve revealed two high-stand periods characterised by relatively continuous stable high water-levels of at least a few decades. These periods of high-stand enabled the formation of alternating detrital and aragonite laminae sequences. The two periods correspond to the Hellenistic-early Roman and the late 19th – early 20th centuries high-stands (Bookman (Ken-Tor) et al., 2004; Fig. 1D). In order to eliminate the long-term climatic influence on the pollen record and to have regularly laminated sediments, these two relatively stable high-stand periods were chosen to be the focus of this study.

2.2. Air-borne pollen calendars

Although several aerobiological studies are available for the Israel-Jordan area, most of them do not provide data regarding the Dead Sea region. Thus, we focussed on pollen calendars prepared in areas under semiarid to arid conditions close to the Dead Sea. Surveys of allergenic airborne pollen data collected on the roof of Tsell Harim hotel (Ein Bokek) at the western coast of the southern Dead Sea and on the roof of the Megilot Regional Council building (Kalya) at the northern part of the Dead Sea (Fig. 1A; Waisel, unpublished report 1, unpublished report 2) were chosen for comparison purposes, as the Ze'elim Plain is located in between and shares semi-arid features with both. Additionally, a flowering calendar (Supplementary Table S1) was composed using the

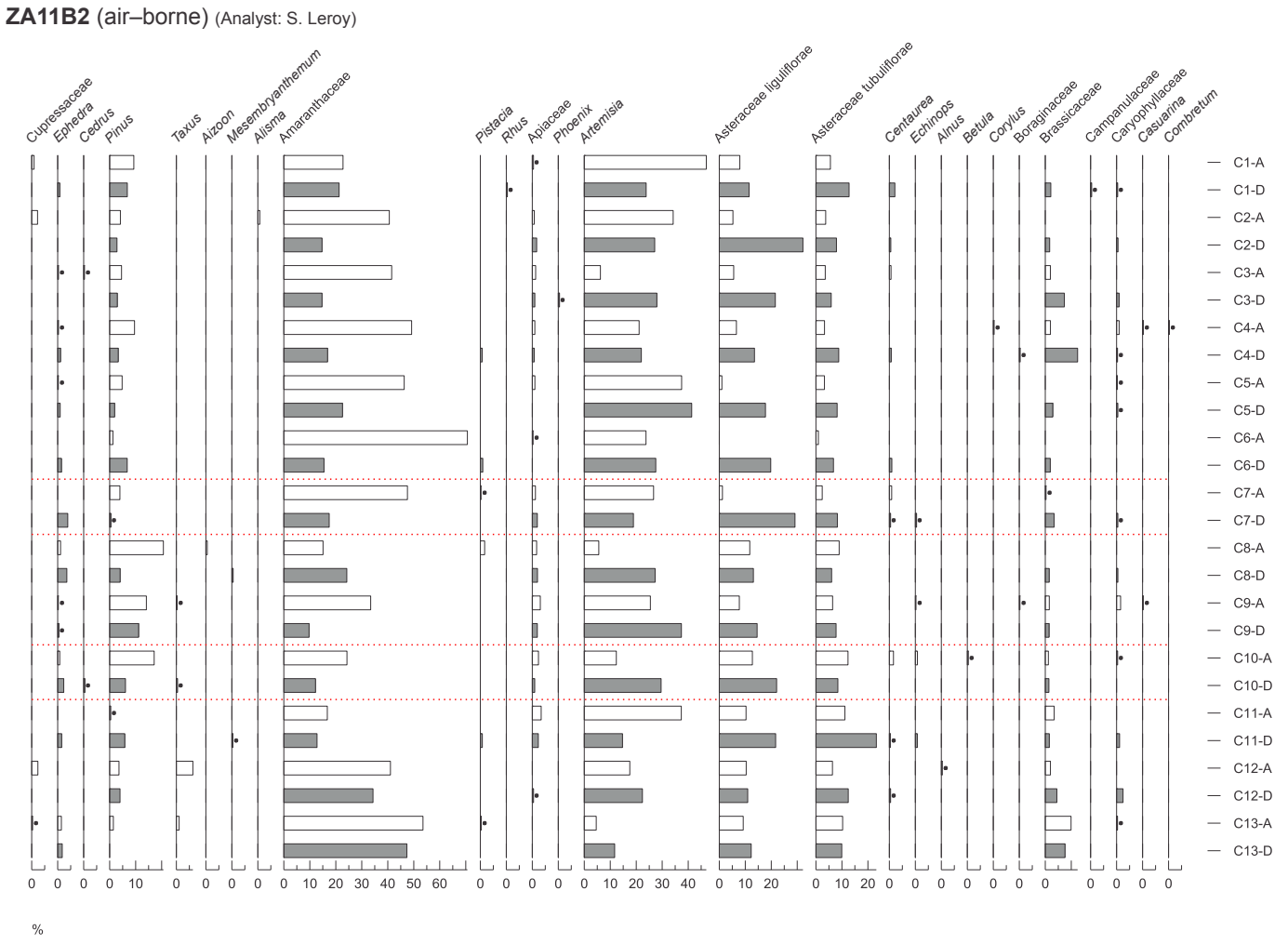

Fig. 4. Percentage diagram of well-preserved pollen (air-borne) of block ZA11B2 (late 19th – early 20th century high-stand). Black dots represent percentages below 0.5%. Red lines separate non-contiguous samples. Detrital laminae are in grey and aragonite laminae in white. Numbers of the detrital-aragonite couplets are as in Supplementary Table S2. (For interpretation of the references to colour in this figure legend, the reader is referred to the web version of this article.)

information contained in the *Handbook of Wildflowers of Israel* (Shmida and Darom, 2000, 2002), paying special attention to the desert and steppe flora, along with the more frequent Mediterranean types in the pollen data.

Reported Ein Bokek and Kalya air-borne data present low total pollen concentrations during the entire year although with a well-defined spring peak. A dominance of Amaranthaceae pollen during the whole year is obvious. Poaceae pollen is also present throughout the year, peaking in spring (March–June). Another characteristic pollen type with large abundance is *Olea*, recorded in April–May at Kalya and in April–May (-June) at Ein Bokek. *Pinus* peaks in March–April in both stations. *Plantago*, another spring bloomer, peaks in March at Kalya and in April at Ein Bokek. An interesting difference between Kalya and Ein Bokek is related to *Artemisia*, which is abundant in Kalya in October–November but almost absent in Ein Bokek, likely because *Artemisia* is a steppe plant and although both Ein Bokek and Kalya are located in the desert, the latter is closer to the steppe area.

Other interesting pollen types that give information on specific flowering periods are infrequent or absent in the aerobiology studies performed in stations close to the Dead Sea. However, they are common in the palaeopalynological studies on Dead Sea Holocene sediments (Baruch, 1993; Heim et al., 1997; Neumann et al., 2007, 2009, 2010; Leroy, 2010; Leroy et al., 2010; Litt et al., 2012; Langgut et al., 2014, 2015a). Brassicaceae and Asteraceae have been identified in March–April in Arad, a town located in the southern Judean Desert (Kantor et al., 1966). Additionally, Brassicaceae species start their flowering period in February in Jerusalem, while Asteraceae species extend their blossom up to May and a few species also bloom in autumn (September–December) (Feinbrun et al., 1959). In fact, the number of Asteraceae and Brassicaceae species is large in Israel, and although many bloom in spring, some of them also flower in autumn (Supplementary Table S1). Arboreal pollen types are representative of long-distance transport to the Dead Sea region. Nonetheless, they are equally informative. *Quercus* is recorded during spring, in March–April mainly (Keynan et al., 1989). Finally, *Pinus* blooming peaks during spring (March–April) as well (Feinbrun et al., 1959).

The use of flowering calendars and palynological analysis to resolve the season in which an event occurred, i.e. a historical earthquake at central Israel (Langgut et al., 2015b), has proven to be reliable in a similar Dead Sea climate context.

2.3. Sampling

The level of the modern Dead Sea is the result of a large human-

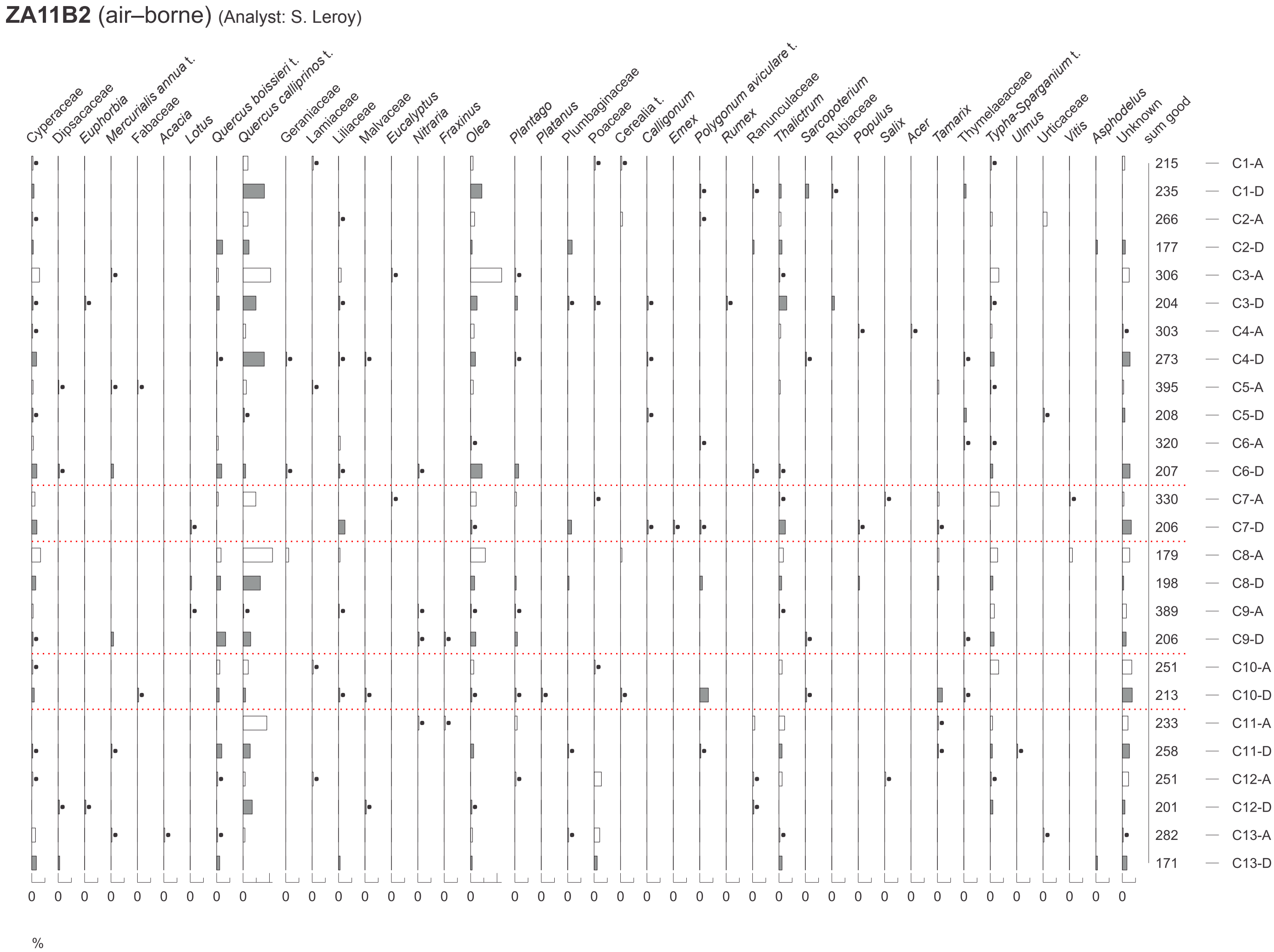

Fig. 4. (*continued*).

induced retreat linked to the damming of its northern tributary (Sea of Galilee) and water pumping for industrial purposes. This retreat has triggered the formation of several meter deep gullies in the Ze'elim Plain (Ben Moshe et al., 2008). Late Holocene laminated sequences are exposed in these gullies (Fig. 1B). The two aforementioned high-stand periods were identified in the radiocarbon-dated outcrop (Bookman (Ken-Tor) et al., 2004; Fig. 1D) in February 2011. One block of laminated sediments from the late 19th – early 20th centuries high-stand (ZA11B2), and three blocks of laminated sediments from the Hellenistic-early Roman high-stand (ZA11B3R, ZA11B4L, ZA11B5L) were collected (Fig. 1D). Sampling of individual, mm-scale laminae was done at the sedimentology laboratory of the University of Haifa using a scalpel. Only consecutive detrital and aragonite laminae with no suspicion of contamination or mixing with the upper and lower layers were considered. Overall, 65 detrital-aragonite couplets (130 samples) were analysed: 13 in block ZA11B2 (couplets 1 to 13), 11 in block ZA11B3R (couplets 14 to 24), 17 in block ZA11B4L (couplets 25 to 41) and 24 in block ZA11B5L (couplets 42 to 65) (Supplementary Table S2).

Additionally, fine mud carried in suspension in flash-floods that occurred between February 2009 and June 2012, was collected from drying puddles immediately after the events. A total of 28 flash-flood samples were analysed (Fig. 1C; Supplementary Table S3).

2.4. Grain-size distribution analysis

Grain-size analysis of the Ze'elim detrital laminae was performed at the University of Haifa using a Beckman-Coulter LS 230 laser particle size analyser over the particle size range of 0.02–2000 μm. Five replicate samples were measured for each detrital lamina. Grain-size was determined after dissolution of carbonate minerals. In block ZA11B4L and in a few samples of block ZA11B2 it was not determined due to low sample mass available (Supplementary Table S2). Additionally, for two thicker detrital laminae, grain-size distribution was measured in sub-samples from the top and bottom parts in order to identify settling patterns.

2.5. Palynological analysis

Palynological extraction was carried out at Brunel University London. Around 0.5–4 ml (usually ~2 ml) of detrital material (detrital laminae and flash-flood samples) and 0.5–12 ml (usually ~5 ml) of aragonite laminae were deflocculated with a $Na_4O_7P_2$ solution (10%). Carbonate dissolution was done with concentrated HCl (35%). Elimination of silicates was obtained by HF (48%) followed by HCl. The residue was sieved through 125 and 10 μm nylon meshes and mounted on slides with glycerol. Concentration estimates (number of palynomorphs/ml of sediment) were calculated

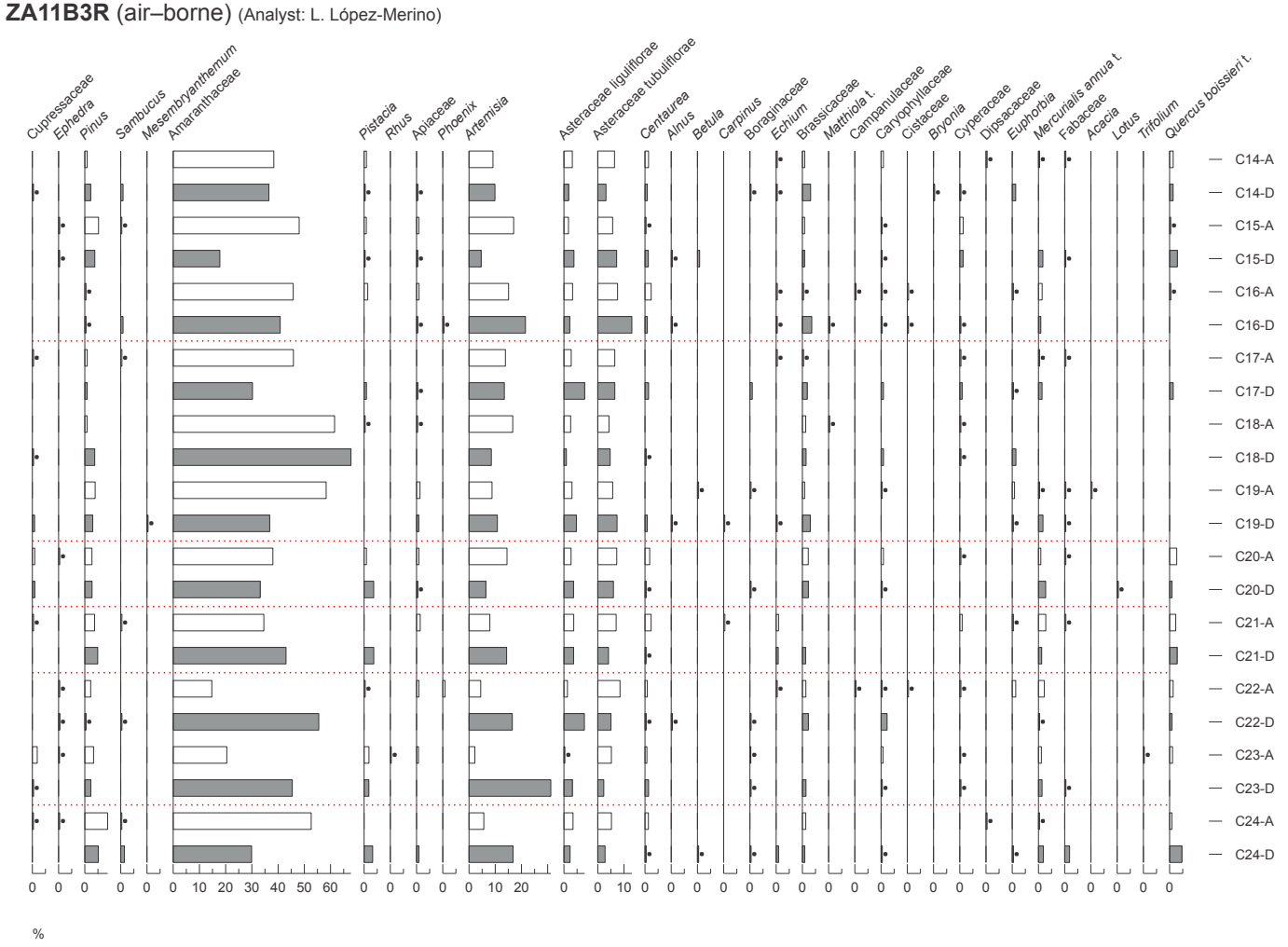

Fig. 5. Percentage diagram of well-preserved pollen (air-borne) of block ZA11B3R (Hellenistic-early Roman high-stand). Black dots represent percentages below 0.5%. Red lines separate non-contiguous samples. Detrital laminae are in grey and aragonite laminae in white. Numbers of the detrital-aragonite couplets are as in Supplementary Table S2. (For interpretation of the references to colour in this figure legend, the reader is referred to the web version of this article.)

based on the addition of *Lycopodium* tablets at the beginning of the chemical treatment (Stockmarr, 1971). Palynological identification and counting was completed on light microscopes at × 400, and at × 1000 using immersion oil for more delicate identifications, and complemented by the Brunel University London pollen reference collection and atlases (Reille, 1992, 1995, 1998). Where possible, a minimum of 200 well-preserved (air-borne), non-reworked, pollen grains were counted per sample (average = 242). Palynological diagrams were elaborated using Psimpoll 4.27 (Bennett, 2009).

As pollen found in southern Dead Sea sediments could be transported by both wind and water run-off (Horowitz et al., 1975; Baruch, 1993), it is necessary to be sure about the air-borne component to be able to detect the timing of laminae deposition. Hence, reworked pollen grains (water-borne) were counted separately form well-preserved (air-borne) pollen grains and classified into different categories: broken, corroded, crumpled, degraded and other reworked (when two or more features were present) (Supplementary Table S1). Broken stamina were grouped with the reworked material. On average, 618 reworked pollen grains were counted per sample. Fungal spores had a significant presence and thus were also quantified. On average, 195 fungal spores were counted per sample. Full counts of reworked pollen grains and fungal spores are given in Supplementary Figs. S2–S6.

The concentration of Total well-preserved pollen grains, Total reworked pollen grains and Total fungal spores were calculated separately. The first includes the well-preserved pollen grains only (number of well-preserved pollen grains per ml of sediment), the second one includes the reworked pollen grains only (number of reworked pollen grains per ml of sediment), and the third includes the fungal spores only (number of fungal spores per mil of sediment).

2.6. Numerical analysis

In order to unravel the seasons in which the laminae could have been deposited, Principal Components Analysis (PCA) was applied to the well-preserved palynological dataset. This approach has been confirmed as valid for detecting seasonality in palaeoenvironmental studies (i.e. Festi et al., 2015). In this case, the PCA has been performed on the transposed well-preserved pollen data matrices (samples in columns as variables, and taxa in rows as cases). This approach enables us to summarise the main palynological assemblages of co-existing taxa and their importance in each sample. Thus, the palynological composition of the samples can be compared based on co-variation patterns (López-Merino et al., 2012). Taxa showing large factor scores (i.e. larger

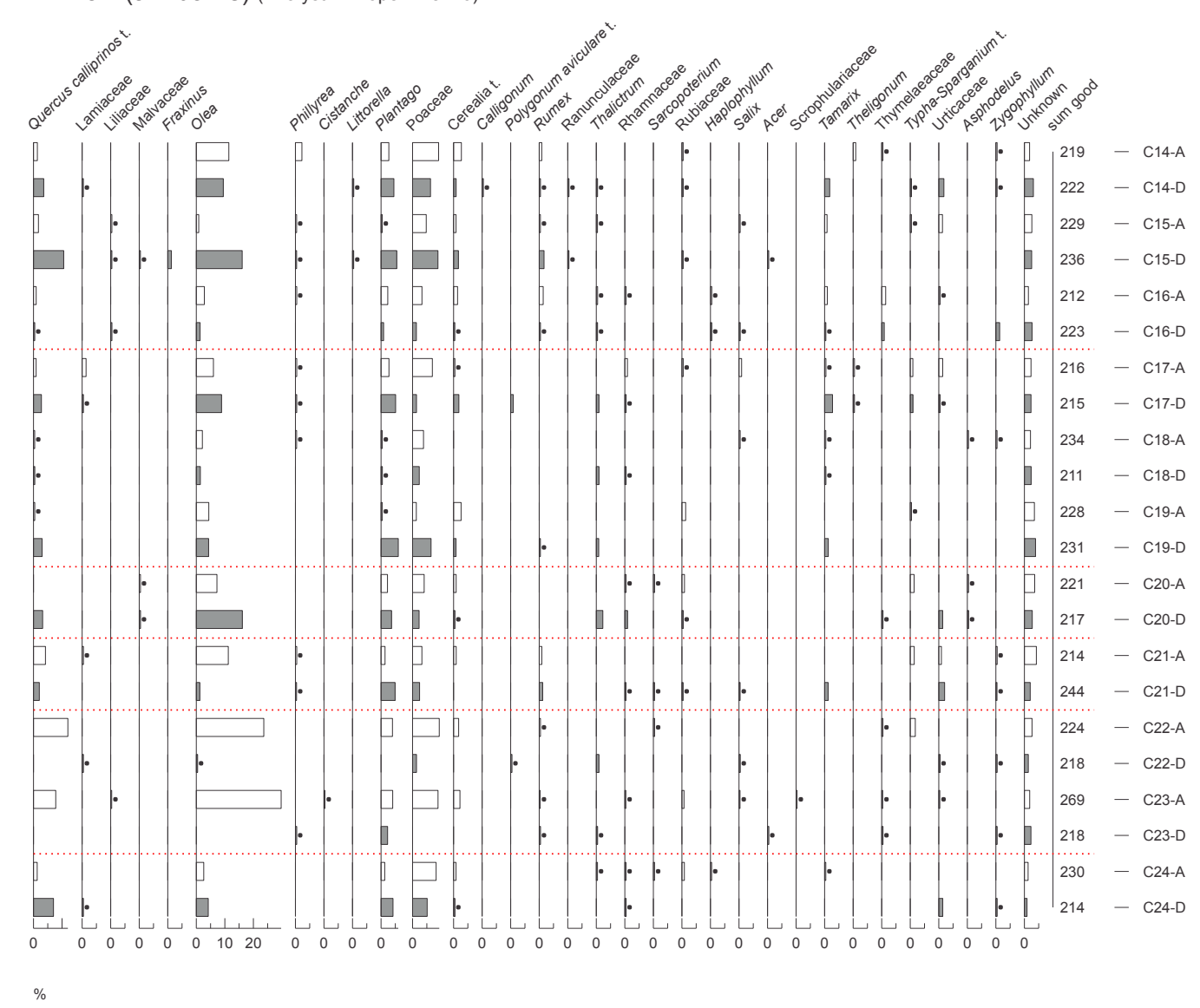

Fig. 5. (*continued*).

abundances) in a given principal component explain most of the variation of the palynological dataset in samples with large factor loadings. This enables quantitative expression of the proportion of variance explained by each principal component for each sample (López-Merino et al., 2012).

Baruch (1993) presented the palynological analysis of 35 surface samples distributed along four vegetation zones of Israel: Mediterranean, transitional and steppe, desert, and the Dead Sea shore. The Mediterranean zone was dominated by arboreal taxa (*Quercus calliprinos*, *Pinus* and *Sarcopoterium spinosum*), the transitional zoned was characterised by *Sarcopoterium spinosum*, Brassicaceae and *Artemisia*, while the desert area was dominated by Brassicaceae and Asteraceae. In the pollen rain in the Dead Sea shore, Amaranthaceae pollen was overrepresented. Therefore, in order to reduce background noise and detect the main characteristic palynological associations, Amaranthaceae pollen was excluded from the analysis. Many species belonging to this pollen type bloom all yearlong and very locally. Therefore, its pollen is overrepresented and dominates the pollen assemblages regardless the season (Baruch, 1993; Waisel, unpublished report 1, unpublished report 2). After the exclusion of Amaranthaceae and prior to the statistical analysis data-set proportions were recalculated. Correlation matrices and varimax rotation solutions were applied to constrain the co-variation in the components. PCA was done using the IBM SPSS statistics 20 software.

3. Results

3.1. Grain-size

The siliciclastic fraction of the detrital laminae showed at least three different grain-size modes. Most samples had two grain-size modes, a first fine mode of 3–10 μm and a second coarser mode of 20–90 μm (Fig. 2). A ~10 μm mode was obtained on samples from collectors installed on a buoy on the Dead Sea surface during three years (1997–1999) (Singer et al., 2003). This grain-size distribution represents dust deposited over the Dead Sea similar to that of long-range transported Harmattan dust (Stahr et al., 1994) and is

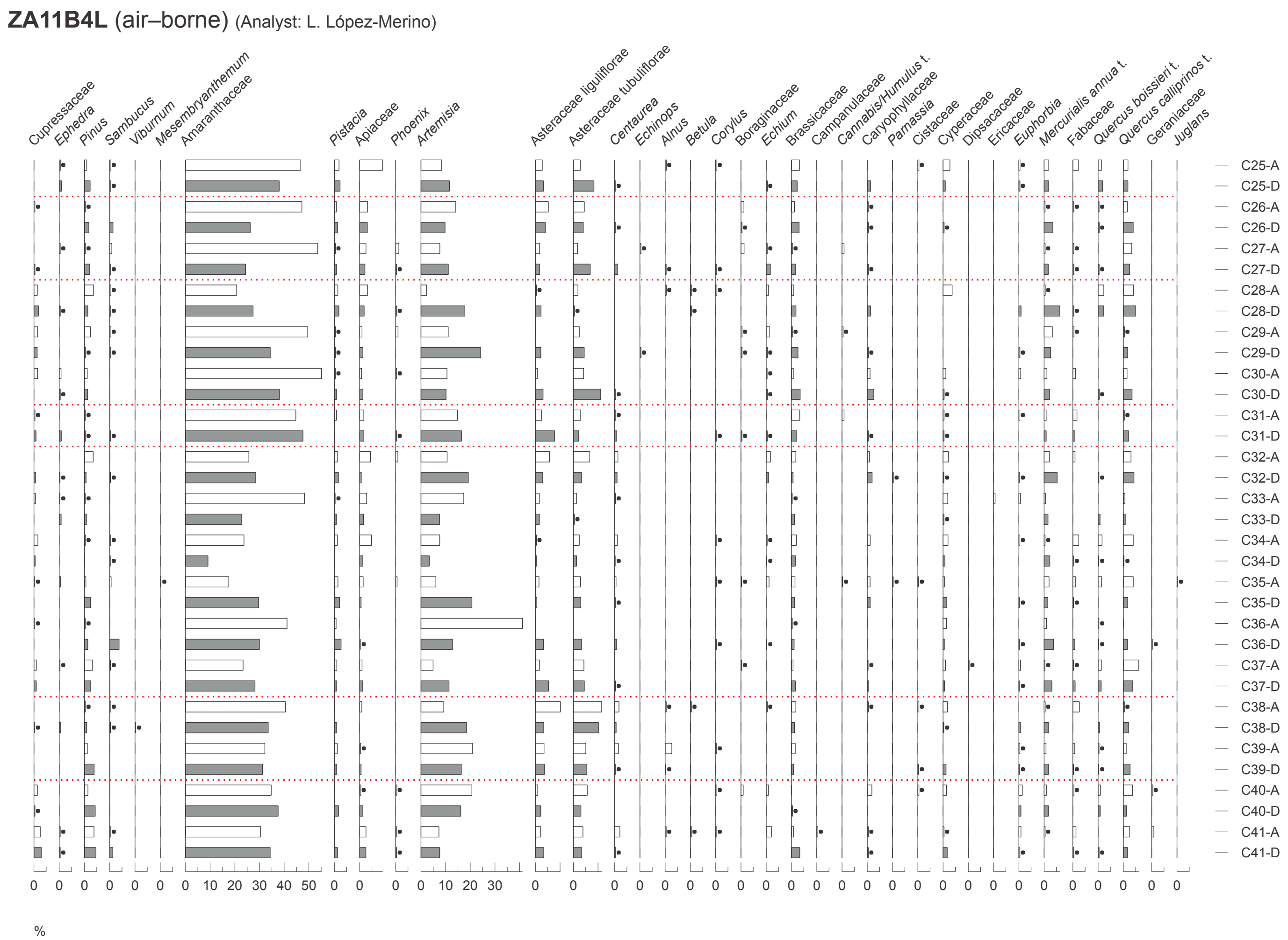

Fig. 6. Percentage diagram of well-preserved pollen (air-borne) of block ZA11B4L (Hellenistic-early Roman high-stand). Black dots represent percentages below 0.5%. Red lines separate non-contiguous samples. Detrital laminae are in grey and aragonite laminae in white. Numbers of the detrital-aragonite couplets are as in Supplementary Table S2. (For interpretation of the references to colour in this figure legend, the reader is referred to the web version of this article.)

comparable to the grain-size distribution of air-borne dust in the Sde Boker area (Negev) (Offer et al., 1992). Thus, the fine grain-size mode in the detrital laminae siliciclastic fraction is consistent with fine dust largely wind-transported from medium to long range. Although a bimodal distribution is in accordance with Haliva-Cohen et al. (2012), the average grain-size measured for the second mode in this study is coarser, possibly due to the carbonate dissolution stage. Few samples included a minor third mode of 100–200 μm (Fig. 2) consistent with the contribution of loess (Haliva-Cohen et al., 2012), likely representing a local source.

The general grain-size distribution measured from detrital laminae suggests it is composed of recycling of local and distal sources as demonstrated in previous studies (e.g. Belmaker et al., 2014). Additionally, grain-size distribution within thicker detrital laminae shows graded bedding that suggests sediment deposition during flash-flood events. This phenomenon was shown with upward fining of the grain-size distribution in specific laminae (Fig. 2D) and was also described in petrographic thin-slides (Haliva-Cohen et al., 2012). The understanding that the detrital laminae consist of both air-borne particles and recycled local (mostly Quaternary sequences) material lead to the conclusion that the palynological analysis should separate air-borne from reworked pollen. This approach is practiced in the Dead Sea sediments at a very fine detail here for the first time.

3.2. Palynology

Two prerequisites are necessary to validate the timing of laminae deposition: (i) detecting features indicative of seasons and (ii) identifying features suggestive of a link between detrital laminae and flash-flood events. These prerequisites were achieved by counting separately poorly-preserved pollen grains (reworked), mainly indicative of water transport and reworking from soils, from well-preserved pollen grains, mostly derived from air-borne transport, hence providing blooming period information.

3.2.1. Air-borne: detecting seasonal features

Well-preserved pollen grains were present in both flash-flood samples (Fig. 3) and detrital-aragonite couplets (Figs. 4–7). Although the number of pollen types identified is high (81 types in the flash-floods, 67 types in ZA11B2, 65 types in ZA11B3R, 70 types in ZA11B4L, and 73 types in ZA11B5L), few pollen types dominate the pollen assemblages. As expected due to the location of the Ze'elim Wadi and fan delta under semi-arid conditions, one of the main pollen types in both detrital and aragonite layers is Amaranthaceae (Baruch, 1993). Other abundant pollen types are

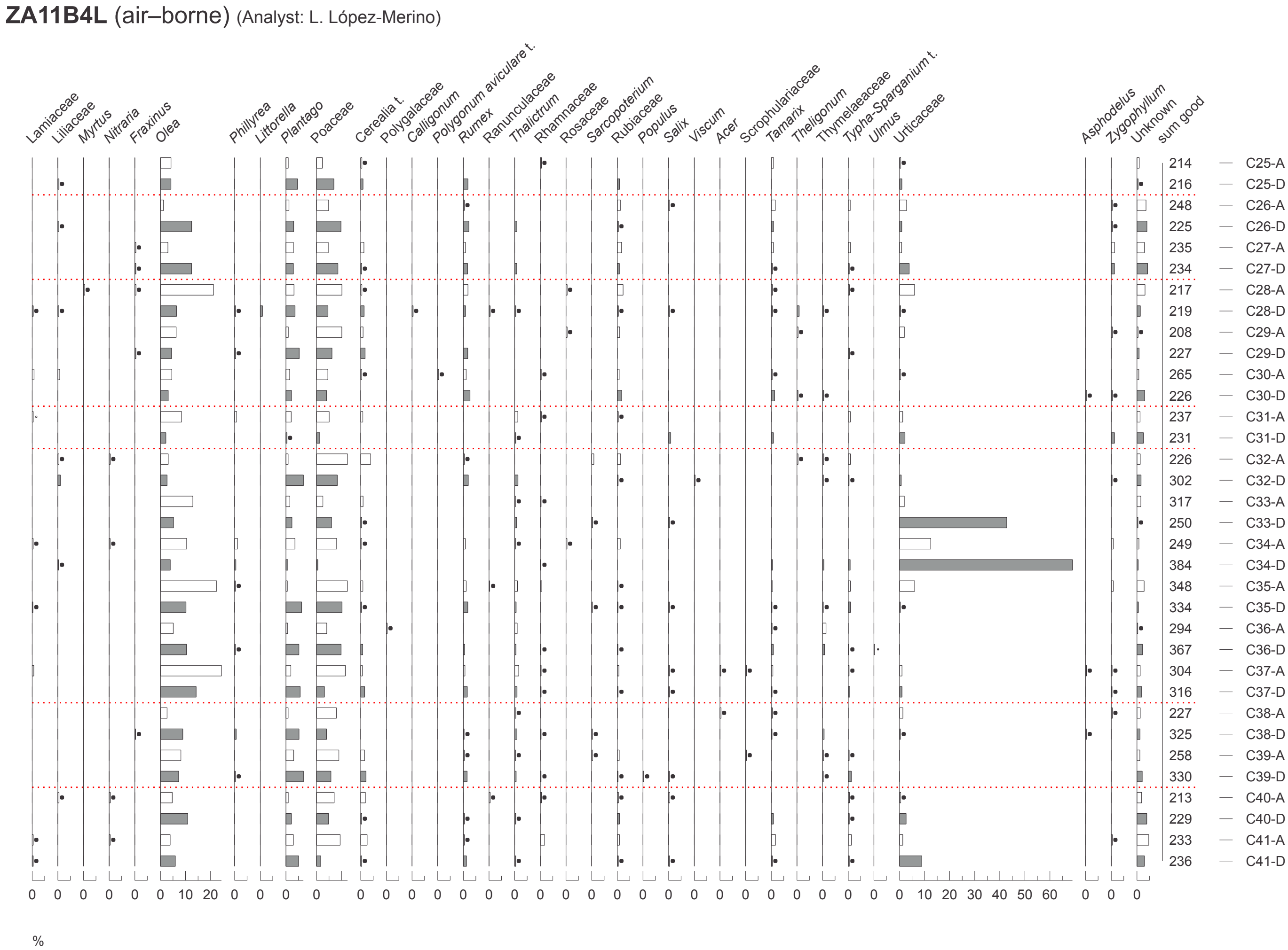

Fig. 6. (*continued*).

Asteraceae liguliflorae, Asteraceae tubuliflorae, *Artemisia*, Brassicaceae, *Quercus calliprinos* t., *Pinus*, *Olea* and Poaceae (Figs. 4–7). Pollen assemblages from recent flash-flood samples show the current highly anthropised landscape with low presence of long-distance Mediterranean arboreal pollen types such as *Quercus* and *Olea*, as well as larger percentages of *Pinus* pollen due to anthropogenic afforestation (Fig. 3). Hence flash-flood samples have not been included in the statistical analysis. A preliminary PCA included samples from both high-stand periods (Hellenistic-early Roman and late 19th – early 20th centuries). PCA results separated the two periods on the basis of *Olea* (ZA11B2 *versus* ZA11B3R, ZA11B4L, ZA11B5L, data not shown). This is consistent with the intense olive tree cultivation during Hellenistic-early Roman times, a period dominated by intense arboriculture, which has no equivalent in the present (Baruch, 1993; Neumann et al., 2007, 2010; Leroy, 2010). Therefore, in order not to conceal differences among detrital and aragonite laminae due to the impact of the higher presence of *Olea* during the older high-stand period, the two high-stand periods were explored separately.

The PCA of the late 19th – early 20th centuries high-stand transposed data matrix resulted in three principal components explaining 93.6% of the total variance in the dataset (Fig. 8). $PC1_{Recent}$ explains 46.9% of the variance, with *Artemisia* commanding the largest positive factor score (Fig. 8). *Artemisia* species in the steppe area bloom in autumn (Supplementary Table S1), particularly in September–October (–November). Hence, $PC1_{Recent}$ seems to be a strong autumn indicator. $PC2_{Recent}$ explains 32.3% of the variance. Asteraceae liguliflorae, Asteraceae tubuliflorae and Brassicaceae present large positive factor scores. *Artemisia* also has a positive score, although moderate. On the other hand, *Pinus*, *Olea*, *Quercus calliprinos* t. and *Typha-Sparganium* t. have negative scores (Fig. 8). Asteraceae and Brassicaceae species are abundant in Israel. Although many of them bloom in spring, some bloom all year-long (Supplementary Table S1) particularly in autumn-winter. The observation that for $PC2_{Recent}$ spring (*Pinus*, *Olea*, *Quercus calliprinos* t.) and late spring-early summer (*Typha-Sparganium* t.) bloomers present negative scores, while the autumn indicator *Artemisia* has a positive score, could be indicative of this principal component as an autumn indicator as well. This is perhaps more related to the direction of winds. Horowitz et al. (1975) pointed out that the origin and routes of winds (e.g. due to dust and rain storms) are an important factor in the pollen provenance. As mentioned above for the surveys of allergenic airborne pollen data at Ein Bokek (southern Dead Sea) and Kalya (northern Dead Sea) (Fig. 1), *Artemisia* is important in autumn at Kalya only, representing the *Artemisia*-dominated steppe ($PC1_{Recent}$). However, *Artemisia* is almost absent at Ein Bokek, representing a more desert-like vegetation like the assemblage separated by $PC2_{Recent}$. $PC3_{Recent}$ explains 14.4% of the variance. *Pinus*, *Quercus calliprinos* t. and *Olea* present large positive factor scores, while Asteraceae tubuliflorae, Asteraceae

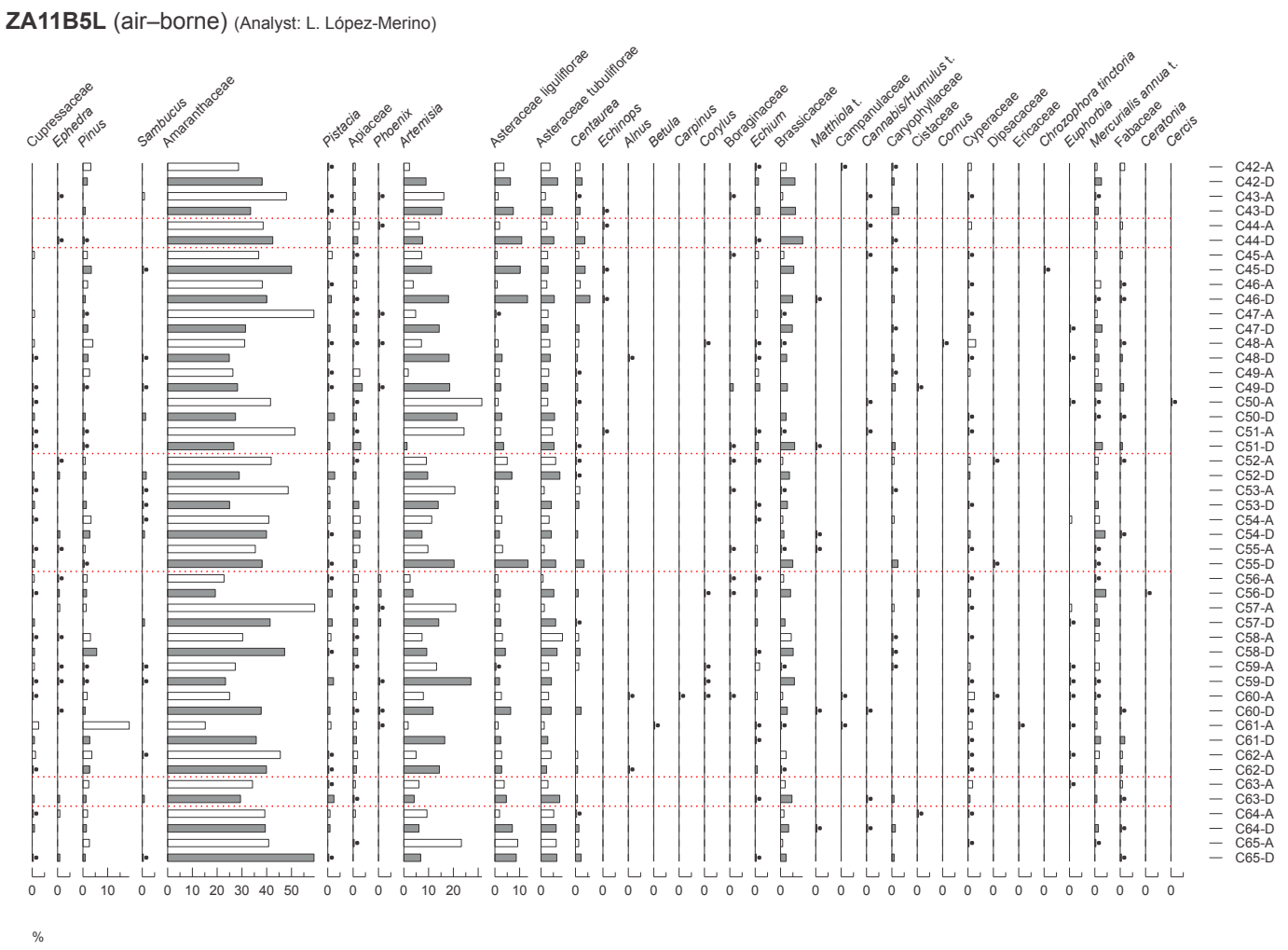

Fig. 7. Percentage diagram of well-preserved pollen (air-borne) of block ZA11B5L (Hellenistic-early Roman high-stand). Black dots represent percentages below 0.5%. Red lines separate non-contiguous samples. Detrital laminae are in grey and aragonite laminae in white. Numbers of the detrital-aragonite couplets are as in Supplementary Table S2. (For interpretation of the references to colour in this figure legend, the reader is referred to the web version of this article.)

liguliflorae and *Typha-Sparganium* t. have more moderate scores (Fig. 8). The flowering period of *Pinus*, *Quercus calliprinos* t. and *Olea* extends from March to May. *Typha-Sparganium* t. flowers in June–July, while most Asteraceae species have their peak period of pollen release from March to June (Supplementary Table S1). Thus, $PC3_{Recent}$ is a strong indicator for spring.

The PCA of the Hellenistic-early Roman high-stand transposed data matrix resulted in five principal components explaining 92.0% of the total variance (Fig. 9). $PC1_{Hellenistc}$ explains 40.8% of the variance, with *Artemisia* accounting for the largest positive factor score (Fig. 9), likely indicating that samples dominated by $PC1_{Hellenistic}$ have an autumn-dominated pollen assemblage as indicated by $PC1_{Recent}$ for the 19th – early 20th centuries sequence. $PC2_{Roman}$ explains 33.3% of the variance, with *Olea* presenting the largest positive factor score, whereas Poaceae, *Quercus calliprinos* t. and *Plantago* show more moderate scores (Fig. 9). The species included within these pollen types are spring bloomers (Supplementary Table S1). Thus, $PC2_{Hellenistic}$ seems to indicate spring in assemblages with large percentages of olive tree, i.e. olive tree crops. $PC3_{Hellenistic}$ accounts for 9.6% of the variance. Asteraceae liguliflorae, Asteraceae tubuliflorae, Brassicaceae and *Centaurea* present large positive factor scores, while Apiaceae, *Artemisia* and *Tamarix* have more moderate positive scores. Poaceae and *Quercus calliprinos* t. present moderate negative scores (Fig. 9). Similar to $PC2_{Recent}$, this palynological assemblage could be related to autumn. $PC4_{Hellenistic}$ explains 5.2% of the total variance, with *Pinus*, Poaceae and *Quercus calliprinos* t. showing large positive factor scores and Asteraceae tubuliflorae, Apiaceae and *Quercus boissieri* t. more moderate positive scores. On the other hand, *Olea* has a negative factor score (Fig. 9). Similar to $PC2_{Hellenistic}$, $PC4_{Hellenistic}$ likely reflects spring, although with an assemblage without olive tree crops. Finally, $PC5_{Hellenistic}$, which accounts for the 3.1% of the total variance only, is directed by Urticaceae (Fig. 9). This principal component, indicative of spring (Supplementary Table S1), is important in few samples only.

Although for the late 19th – early 20th centuries high-stand, some couplets present an autumn-detrital ($PC1_{recent}$ and $PC2_{recent}$) and a spring-aragonite ($PC3_{recent}$) deposition, most of the variance of the detrital-aragonite couplets is explained by $PC1_{recent}$ and $PC2_{recent}$, pointing at an autumn deposition of the entire couplet (Fig. 10). For the Hellenistic-early Roman high-stand, many detrital-aragonite couplets present an autumn-detrital ($PC1_{Hellenistic}$, $PC3_{Hellenistic}$) and a spring-aragonite ($PC2_{Hellenistic}$, $PC4_{Hellenistic}$ and $PC5_{Hellenistic}$) deposition, while many other couplets present deposition in either autumn or spring (Fig. 10). Furthermore, eight couplets suggested a spring-detrital and a following autumn-

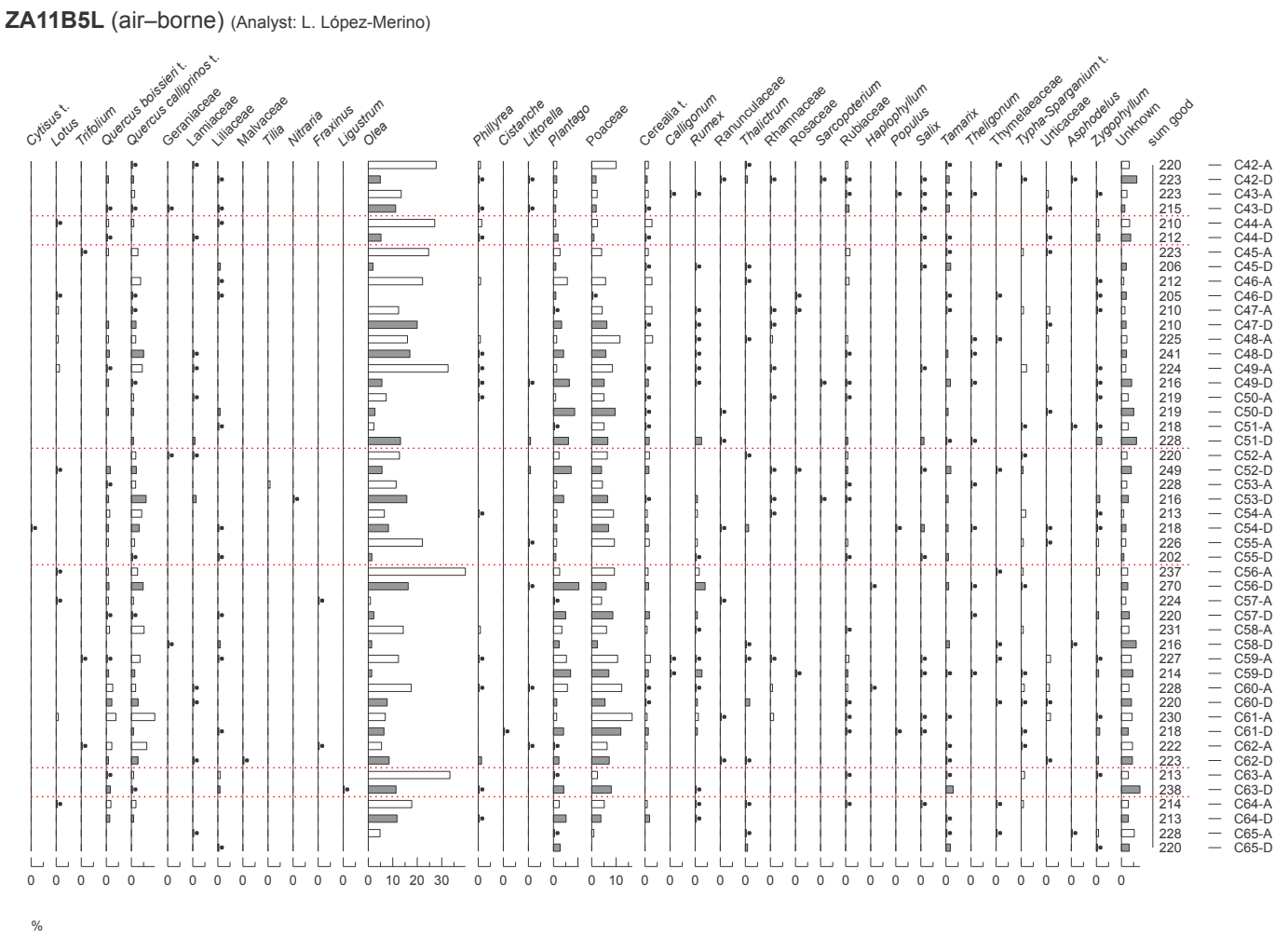

Fig. 7. (*continued*).

aragonite deposition. This result appears in the 12.3% of the couplets only (8 out of 65), and it is difficult to explain, likely pointing to an anomalous result that may be related to contamination from adjacent laminae that was introduced during the difficult sampling of the mm-scale alternating laminae. Further deliberation on the meaning of seasonal deposition will be presented in the discussion.

3.2.2. Water-borne: linking detrital layers with flash-flood events

The concentration of well-preserved pollen grains is usually higher in detrital laminae and flash-flood samples than in aragonite laminae, although the differences are much larger when comparing the concentration of reworked grains (Fig. 11). Aragonite laminae have considerably much lower concentration of reworked pollen grains than detrital laminae and flash-floods samples (Fig. 11; Supplementary Figs. S2–S6). This suggests that water-transported reworked pollen is more significant than wind-transported reworked pollen (which can be the main source of reworking in aragonite layers). The concentration of fungal spores is also lower in aragonite than in detrital and flash-flood samples (Supplementary Figs. S2–S6). The combined concentrations of reworked pollen and fungal spores can be used to assess the link between the formation of detrital laminae and flash-flood events (Fig. 12). Flash-flood and detrital samples present similar log-log distributions with a stronger overlap than flash-floods and aragonite laminae, the latter having lower reworked and fungal spores concentrations and no clear distribution pattern (Fig. 12).

4. Discussion

4.1. The timing of detrital-aragonite deposition

If Dead Sea laminae were varves in the way assumed by some authors, pollen spectra in aragonite laminae would correspond always to summer bloomers, while in detrital layers would have to correspond to autumn-winter-spring pollen assemblages. However, our palynological analysis shows that the air-borne component presents a more complex picture for the timing of aragonite deposition. Furthermore, the detailed palynological examination of the deposition season of detrital-aragonite couplets suggests three possible scenarios (Fig. 10):

- Scenario (i): both detrital and the following aragonite lamina have autumn palynological assemblages (27 out of 65 couplets, 41.5%),
- Scenario (ii): both detrital and the following aragonite lamina have spring palynological assemblages (9 out of 65 couplets, 13.8%), and
- Scenario (iii): the detrital lamina has an autumn palynological assemblage and the following aragonite lamina a spring one (21 out of 65 couplets, 32.3%).

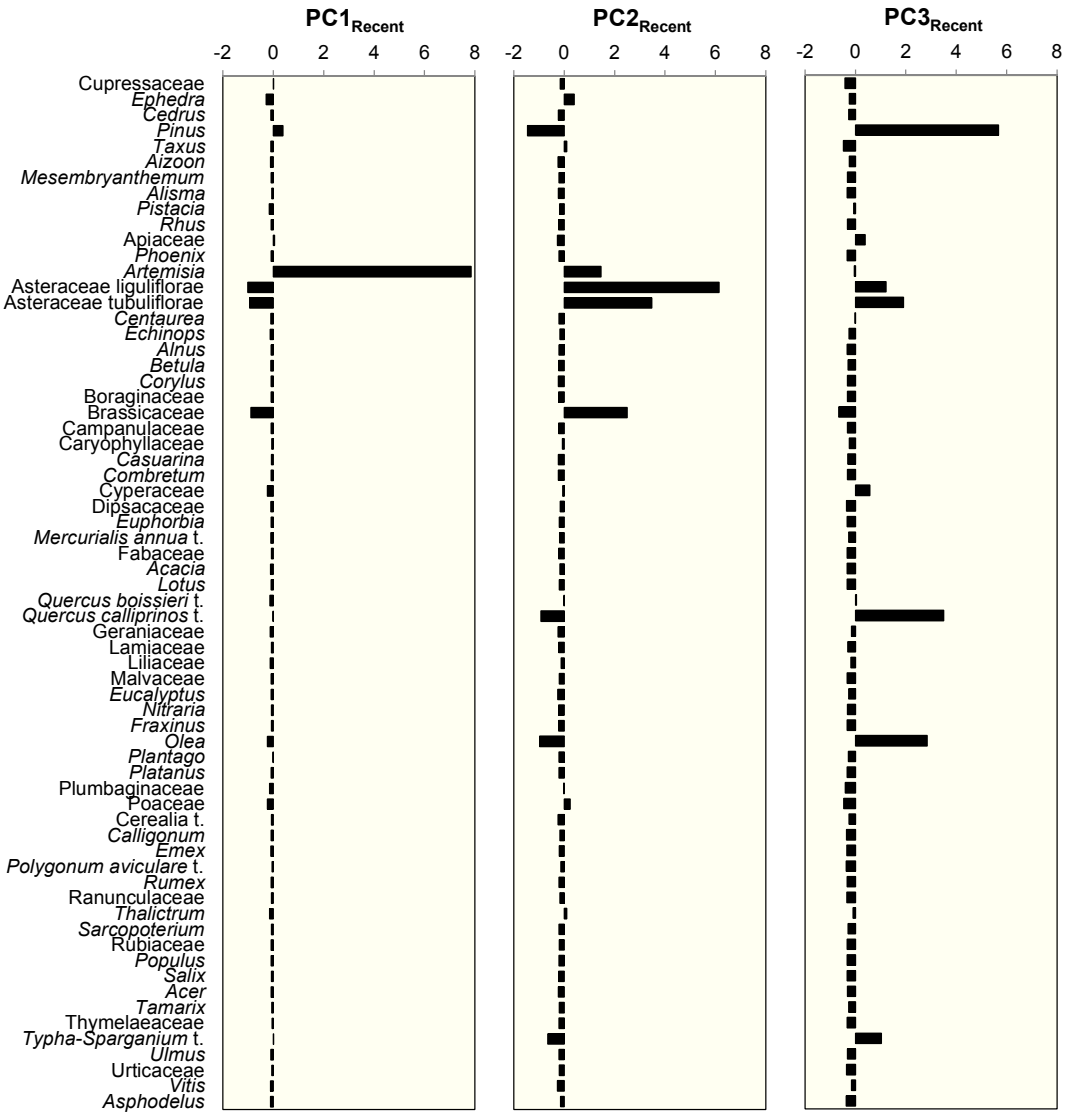

Fig. 8. Factor scores of the three principal components (transposed matrix) obtained for the air-borne component of the late 19th – early 20th centuries high-stand samples (block ZA11B2).

These scenarios show no summer pollen assemblages in the aragonite laminae. One may argue that the lack of summer pollen results from the relatively low dust flux during this season (Singer et al., 2003). However, considering the rapid deposition of aragonite laminae along with the abundance of autumn pollen assemblages this argument does not stand. Thus, we conclude that the deposition of aragonite did not depend exclusively on evaporation and warming of surface waters (Neev and Emery, 1967). This indicates that aragonite precipitation occurred always during the rainy season, either at the same season of the detrital laminae deposition (scenarios i and ii) or during the following spring (scenario iii). These scenarios suggest that the deposition of aragonite laminae requires higher carbonate alkalinity in the flash-flood, hence enabling aragonite saturation without evaporation (Barkan et al., 2001).

Several of the consecutive couplets analysed showed a deposition within the same season (Fig. 10). On the one hand, consecutive autumn pollen assemblages were observed in the following couplets of the late 19th – early 20th century high-stand (block ZA11B2): couplets 13, 12 and 11; couplet 9 and the detrital layer of couplet 8; couplets 6, 5 and 4 and the detrital layer of couplet 3; and couplets 2 and 1. In the Hellenistic-early Roman high-stand consecutive autumn pollen assemblages were observed in a) couplets 19, 18 and 17 in block ZA11B3R; b) couplets 39 and 38; couplet 36 and the detrital layer of couplet 35; and couplets 30 and 29 and the detrital layer of couplet 28 in block ZA11B4L; and c) couplet 50 and the detrital layer of couplet 49; and couplet 43 and the detrital layer of couplet 42 in block ZA11B5L (Fig. 10). On the other hand, consecutive spring pollen assemblages were observed in the aragonite layer of couplet 35 and couplet 34 in block ZA11B4L; and in the aragonite layer of couplet 48 and couplet 47 in block ZA11B5L (Fig. 10).

These short deposition sequences do not allow us to determine whether they were deposited during the same year (i.e. a year with more flash-flood events) or during consecutive years in the same season. The compilation of the annual distribution of flash-floods in five Dead Sea stations (Supplementary Fig. S7) shows the occurrence of flash-flood events from October to May mainly, with few events in June and September. Thus, the modern flash-floods record shows that both situations are possible. However, more than one

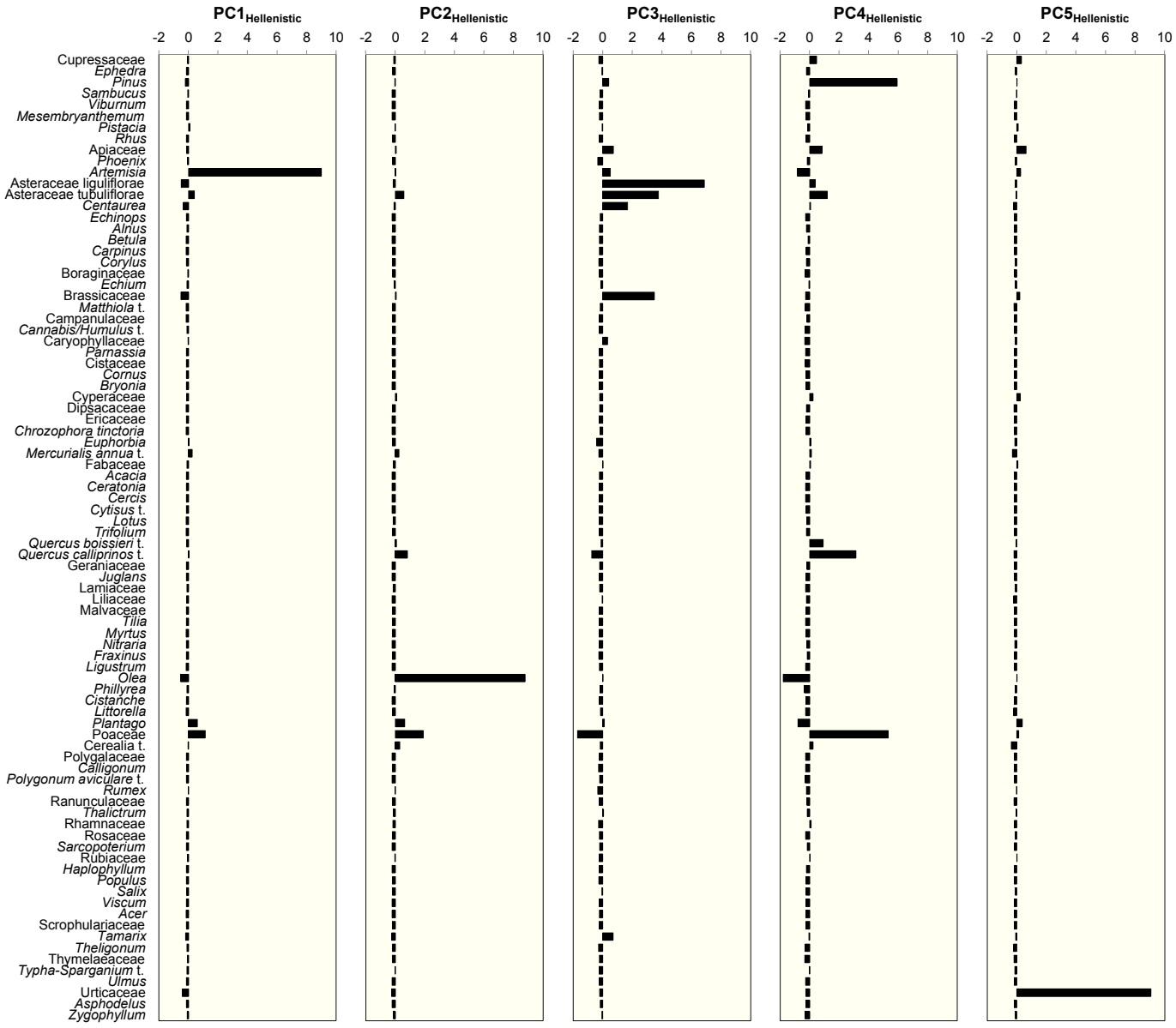

Fig. 9. Factor scores of the five principal components (transposed matrix) obtained for the air-borne component of the Hellenistic-early Roman high-stand samples (blocks ZA11B3R, ZA11B4L and ZA11B5L).

event a season is highly probable in the large drainages (Supplementary Fig. S7). In fact, the palynological assemblages obtained in this study for both detrital and aragonite laminae are those of the rainy season, i.e. when flash-floods are more likely to occur.

Scenario (iii), when a detrital lamina is deposited in autumn and the following aragonite one in spring, agrees with an aragonite precipitation due to mixing of flood freshwater with Dead Sea brine during the rainy season. However, in contrast to scenarios (i) and (ii), the laminae from the same couplet are deposited in different seasons within the rainy period. This scenario may also indicate a longer lag period between the freshwater arrival to the Dead Sea and the chemical deposition. The lacustrine conditions that can lead to this situation are only estimated at this stage. However, the need for sufficient accumulation of dissolved bicarbonate in the lake surface water or the effect of turbulence on chemical deposition is hypothesised as possibly critical in this interpretation.

The analyses performed in this study present for the first time direct evidence for the timing of laminae deposition in the DSB. The abovementioned scenarios suggest that both detrital and aragonite laminae were deposited in a varying seasonal patterns rather than in a strict annual cycle. Detrital layers present grain-size distributions composed of sediment recycling of rock and sediment outcrops in the Dead Sea watershed and distal sources by aeolian transport. These recycled sediments reach the Dead Sea via run-off or as direct dust deposition from the atmosphere. Run-off sediment transport as the main process is confirmed by the large presence of reworked pollen grains and fungal spores (water-borne component) in the detrital laminae compared to the aragonite laminae (Fig. 12). Erosion of soils delivered reworked pollen and fungal spores with the sediments that deposited within the detrital laminae. Aragonite precipitates from the upper surface water layer due to mixing of flood-water with Dead Sea brine (Stein et al., 1997; Barkan et al., 2001).

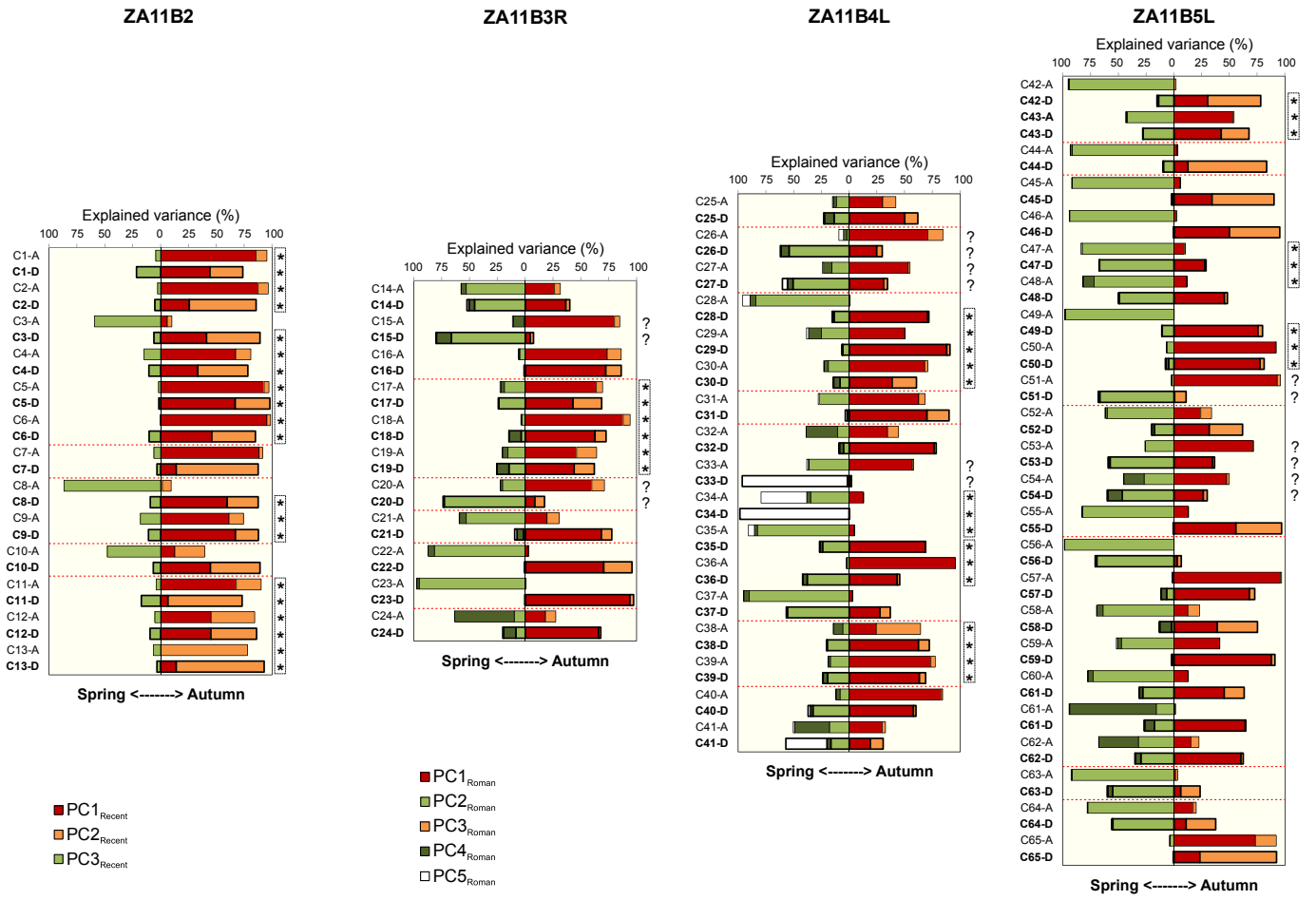

Fig. 10. Percentage of explained variance (square of factor loadings x 100) of the principal components extracted for the late 19th – early 20th centuries high-stand samples ($PC1_{Recent}$, $PC2_{Recent}$ and $PC3_{Recent}$) and the Hellenistic-early Roman high-stand samples ($PC1_{Hellenistic}$, $PC2_{Hellenistic}$, $PC3_{Hellenistic}$, $PC4_{Hellenistic}$ and $PC5_{Hellenistic}$). Proportion of variance that can be explained by the extracted principal components (communalities) is shown for each lamina. The graphs can be read as a sequence of laminae deposition (detrital and following aragonite), with the percentage of the variance explained by the principal components with autumn palynological assemblages plotting to the right and by the principal components with spring palynological assemblages plotting to the left. Asterisks (*) highlight the laminae in which it is possible that more than one detrital-aragonite couplet have been deposited in one year. Question marks (?) highlight the eight couplets with an anomalous result likely due to contamination during sampling. Red lines separate non-contiguous samples. Numbers of the detrital-aragonite couplets are as in Supplementary Table S2. (For interpretation of the references to colour in this figure legend, the reader is referred to the web version of this article.)

This study indicates that, in contrast to previous assumptions, detrital-aragonite couplets were deposited during the rainy season as a result of flash-flood events, hence Dead Sea laminated sediments cannot be considered as varves. This result is of great importance for the accurate use of the DSB laminated sequences as palaeoenvironmental and paleoclimate archives (e.g. the ICDP Dead Sea Deep Drilling Project), and it delivers exciting new information to the Dead Sea scientists and the palaeoclimate community alike.

4.2. Palaeoenvironmental implications and further research

During a flood event, water entering the Dead Sea is dispersed in a plume that floats over the dense saline waters (Nehorai et al., 2013). The suspended sediment in the plume ultimately deposits on the lake bottom. Plume sediment dispersal is a function of flood discharge, wave energy and distance from the shore. Consequently, the central deep part of the basin will record fewer flash-flood events as compared to the margin. In addition, the potential problem of reworking of deposited sediment destroying depositional laminations has to be taken into account. This may prevent, with the uncertainty of having more than one couplet deposited per year, the use of the detrital-aragonite couplets for laminated-based chronologies, i.e. if the laminated-based chronology of a studied sediment core is of long duration the number of couplets per time-unit may vary due to variations in the shore distance or/and flash-flood discharge. In addition, larger discharge carrying more sediment will deposit thicker and coarser detrital laminae. On the other hand, the higher the lake level the further the deposition location from the shore. This yields thinner and finer grain-size laminae. In brief, both parameters are climatically controlled, but result in a reverse effect on the deposition character of the detrital laminae, preventing the use of the thickness and grain-size of the laminae as a direct climatic indicator.

Barkan et al. (2001) pointed out that the aragonite precipitation rate calculated by Stein et al. (1997) for the laminated sediments of the Lisan Formation required a run-off influx six-fold higher than the contemporary run-off influx. Thus, indicating that the Lisan period was more humid than nowadays and that flash-flood events could have been more pronounced. Stein et al. (1997), however, based on previous reports (Neev and Emery, 1967; Begin et al., 1974), interpreted the aragonite formation as precipitation due to increased evaporation in summer. Therefore, understanding the deposition processes of the laminated sediments is of considerable importance for palaeoenvironmental reconstructions. This work

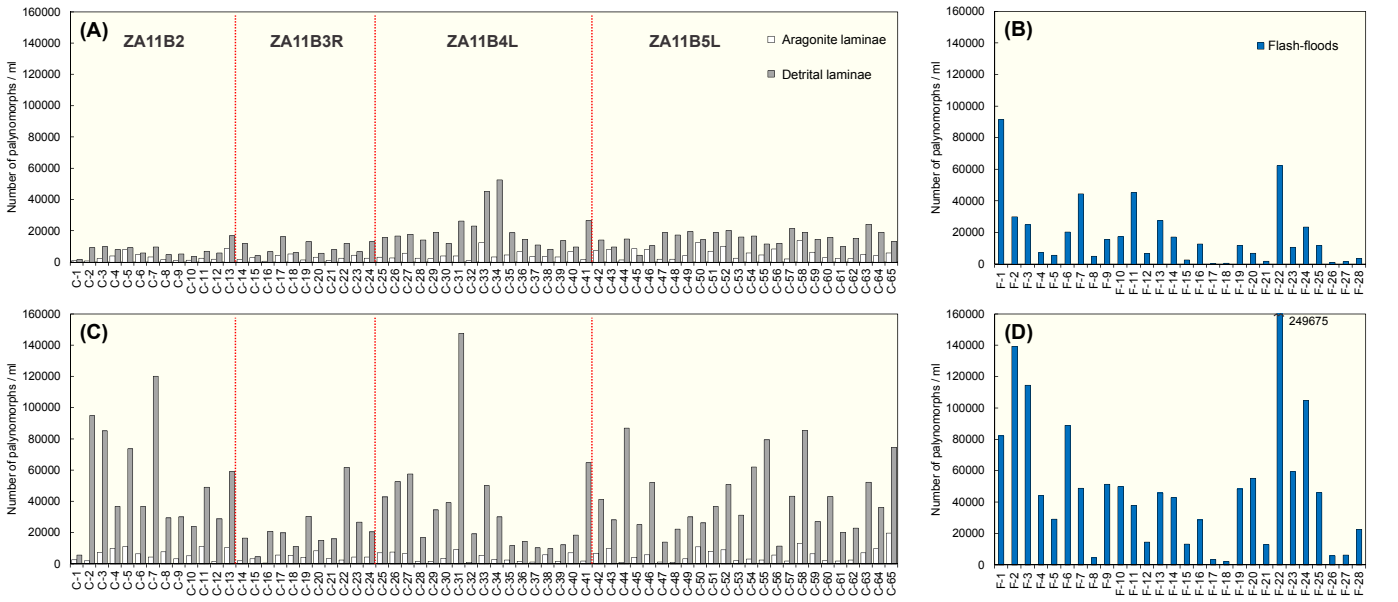

Fig. 11. (A) Concentration of Total well-preserved pollen grains in the Ze'elim detrital-aragonite couplets. (B) Concentration of Total well-preserved pollen grains in modern flash-flood samples. (C) Concentration of Total reworked pollen grains in the Ze'elim detrital-aragonite couplets. (D) Concentration of Total reworked pollen grains in the modern flash-flood samples. Numbers of the detrital-aragonite couplets are as in Supplementary Table S2. Numbers of the flash-flood samples are given in Supplementary Table S3.

has provided the first palynological evidence for unravelling the timing of aragonite laminae deposition, which has been identified as occurring during the rainy season rather than summer, but further research is necessary.

5. Conclusions

This research attempts to identify by palynology the timing of the Dead Sea laminae deposition. Our results demonstrate that:

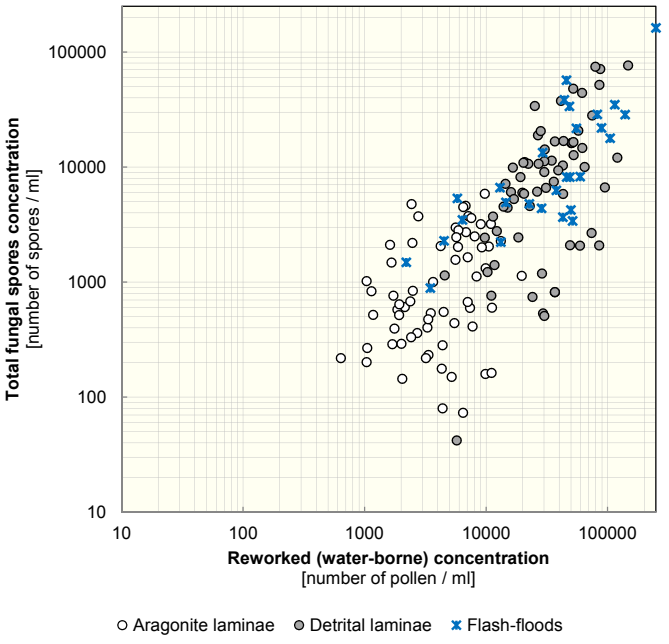

Fig. 12. Concentration of Total reworked pollen grains (water-borne) versus Total fungal spores for detrital and aragonite laminae in the Ze'elim outcrop and contemporary flash-flood samples.

1. Couplets are not necessarily deposited with annual cyclicity. The air-borne component is more complex than a rainy season-detritus *versus* a summer-aragonite deposition, as all laminae presented pollen assemblages representative of the rainy season.
2. The concentration of reworked pollen grains in detrital layers and flash-flood samples is similar and much higher than in aragonite layers. Palynological concentration of reworked grains compared with fungal spores, which represent erosion and soil products, separated detritus and flash-flood samples from aragonite ones.
3. Grain-size distribution indicates that detrital laminae are composed of recycling of local and distal sources, with coarser particles deposited in the Dead Sea watershed and later transported via run-off to the lake.
4. Aragonite precipitation from the upper surface water layer does not necessarily require evaporation and warming of surface waters.

The conclusions drawn above suggest that detrital-aragonite couplets in the Dead Sea laminated sediments are most likely not varves and that the laminae deposition is related to the occurrence of flash-flood events. Whether for specific rainfall patterns (i.e. one flood a year, which is very unlikely) those laminae could provide annual information or not is something that needs to be further tested in other Dead Sea contexts, likely in long and undisturbed laminated sections with many continuous laminae such as the Lisan upper member (i.e. Prasad et al., 2004) and the Ein Feshkha sequences (Kagan et al., 2011).

Further research is necessary to understand whether the number of couplets formed due to flash-flood events depends on the distance from the shoreline, meaning that sediments sections covering the same chronology from different parts of the DSB (shoreline *versus* deep basin) could have different number of laminations. Hence, laminae counting as dating tool of Dead Sea sediments should be re-evaluated. However, these laminated sequences should be used for the reconstruction of palaeo-flash flood records that will have a significant impact on

understanding the palaeo-hydrology of the DSB and its implication to high-resolution climatic interpretation.

Acknowledgements

This research was made possible through the support of the British Council's Britain-Israel Research and Academic Exchange Partnership (BIRAX), which aims to further institutional links between universities in the UK and Israel, awarded to S.A.G. Leroy and R. Bookman and entitled "Resolving the deposition pattern of the Dead Sea laminae and its implication for understanding hydro-climatic short-term variations in the Levant" (BY2/GEO/08), and partly by an Israel Science Fund grant (ISF, Grant # 1093/10) to R. Bookman. L. López-Merino was first supported by a post-doctoral fellowship (Spanish Government) at Brunel University London and later by the Brunel MINT Scheme. We thank the valuable help of Amanda Rozeik (Brunel University London) with the palynological extraction, and Uri Sha'anan and Dr Nimer Taha (University of Haifa) with the grain-size analysis and the sampling of flash-floods. We are indebted to Professor Antonio Martínez Cortizas (University of Santiago de Compostela) and Dr Stephen Kershaw (Brunel University London) for their perceptive comments on earlier drafts.

Appendix A. Supplementary data

Supplementary data related to this article can be found at http://dx.doi.org/10.1016/j.quascirev.2016.03.024.

References

Barkan, E., Luz, B., Lazar, B., 2001. Dynamics of the carbon dioxide system in the Dead Sea. Geochimica Cosmochimica Acta 65 (3), 355–368.
Baruch, U., 1993. The Palynology of Late Quaternary Sediments of the Dead Sea. Unpublished PhD Dissertation. Hebrew University of Jerusalem, Jerusalem. Hebrew with English abstract.
Begin, Z.B., Ehrlich, A., Nathan, Y., 1974. Lake Lisan – the Pleistocene Precursor of the Dead Sea. Geological Survey of Israel, Bulletin No. 63, pp. 1–30.
Belmaker, R., Lazar, B., Stein, M., Beer Jürg, B., 2011. Short residence time and fast transport of fine detritus in the Judean Desert: clues from ^{7}Be in settled dust. Geophys. Res. Lett. 38 (16), L16714.
Belmaker, R., Stein, M., Beer, J., Christl, M., Fink, D., Lazar, B., 2014. Beryllium isotopes as tracers of Lake Lisan (last glacial Dead Sea) hydrology and the laschamp geomagnetic excursion. Earth Planet. Sci. Lett. 400, 233–242.
Ben Moshe, L., Haviv, I., Enzel, Y., Ziberman, E., Matmon, A., 2008. Incision of alluvial channels in response to a continuous base level fall: field characterization, modeling, and validation along the Dead Sea. Geomorphology 93 (3–4), 524–536.
Bennett, K.D., 2009. Documentation for Psimpoll 4.27 and Pscomb 1.03. C Programs for Plotting Pollen Diagrams and Analysing Pollen Data. The ^{14}Chrono Centre, Archaeology and Palaeoecology. Queen's University of Belfast, Belfast, UK. Available at: http://www.chrono.qub.ac.uk/psimpoll/psimpoll.html.
Bookman (Ken-Tor), R., Enzel, Y., Agnon, A., Stein, M., 2004. Late Holocene lake levels of the Dead Sea. Geol. Soc. Am. Bull. 127 (1–2), 555–571.
Bookman, R., Bartov, Y., Enzel, Y., Stein, M., 2006. Quaternary lake levels in the Dead Sea basin: two centuries of research. Geol. Soc. Am. Special Pap. 401, 155–170.
Dayan, U., Morin, E., 2006. Flash flood-producing rainstorms over the Dead Sea: a review. Geol. Soc. Am. Special Pap. 401, 53–62.
Dayan, U., Sharon, D., 1980. Meteorological parameters for discriminating between widespread and spotty storms in the Negev. Isr. J. Earth Sci. 29, 253–256.
Dayan, U., Ziv, B., Shoob, T., Enzel, Y., 2007. Suspended dust over South-Eastern Mediterranean and its relation to atmospheric circulations. Int. J. Climatol. 24, 1001–1011.
Enzel, Y., Bookman (Ken-Tor), R., Sharon, D., Gvirtzman, H., Dayan, U., Ziv, B., Stein, M., 2003. Late Holocene climates of the Near East deduced from Dead Sea level variations and modern regional winter rainfall. Quat. Res. 60 (3), 263–273.
Feinbrun, N., Rahat, A., Tas, J., 1959. Further studies in atmospheric pollen in Jerusalem. Bull. Res. Counc. Isr. 8D, 31–40.
Festi, D., Kofler, W., Bucher, E., Carturan, L., Mair, V., Grabielli, P., Oeggl, K., 2015. A novel pollen-based method to detect seasonality in ice cores: a case study from the Ortles glacier, South Tirol, Italy. J. Glaciol. 61 (229), 815–824.
Ganor, E., Foner, H., 1996. The mineralogical and chemical properties and the behavior of aeolian Saharan dust over Israel. In: Guerzoni, S., Chester, R. (Eds.), The Impact of Desert Dust across the Mediterranean. Kluwer Academic Publishers, Dordrecht, pp. 163–172.
Greenbaum, N., Ben-Zvi, A., Haviv, I., Enzel, Y., 2006. The hydrology and paleohydrology of the Dead Sea tributaries. Geol. Soc. Am. Special Pap. 401, 63–93.
Haliva-Cohen, A., Stein, M., Goldstein, S.L., Sandler, A., Starinsky, A., 2012. Sources and Transport Routes of Fine Detritus Material to the Late Quaternary Dead Sea Basin.
Heim, C., Nowaczyk, N.R., Negendank, J.F.W., Leory, S.A.G., Ben-Avraham, Z., 1997. Near east desertification: evidence from the Dead Sea. Naturwissenschaften 84, 398–401.
Horowitz, A., Weinstein, M., Ganor, E., 1975. Palynological determination of dust storms provenances in Israel. Pollen spores 17 (2), 223–231.
Kagan, E., Stein, M., Agnon, A., Neumann, F., 2011. Intrabasin paleoearthquake and quiescence correlation on the late Holocene Dead Sea. J. Geophys. Res. 116 (B4). B04311.
Kantor, S.Z., Frank, M., Hoch-Kantor, D., Barkai-Golan, R., Marian, D., Schachnner, E., Kessler, A., de Vries, A., 1966. Airborne allergens and clinical response of asthmatics in Arad, a new town in a desert area in Israel. J. Allergy 37 (2), 65–74.
Katz, A., Kolodny, N., 1989. Hypersaline brine diagenesis and evolution in the Dead Sea-Lake Lisan system (Israel). Geochem. Cosmochimica Acta 53 (1), 59–67.
Ken-Tor, R., Agnon, A., Enzel, Y., Stein, M., Marco, S., Negendank, J.F.W., 2001a. High-resolution geological record of historic earthquakes in the Dead Sea basin. J. Geophys. Res. 106 (B2), 2221–2234.
Ken-Tor, R., Stein, M., Enzel, Y., Agnon, A., Marco, S., Negendank, J.F.W., 2001b. Precision of calibrated radiocarbon ages of historic earth quakes in the Dead Sea Basin. Radiocarbon 43 (3), 1371–1382.
Keynan, N., Waisel, Y., Shomer-Ilan, A., Tamir, R., 1989. Forecasting pollen pollution: correlation with floral development. Ann. Allergy 63, 417–420.
Langgut, D., Neumann, F.H., Stein, M., Wagner, A., Joy, Kagan, E.J., Boaretto, E., Finkelstein, I., 2014. Dead Sea pollen record and history of human activity in the judean highlands (Israel) from the Intermediate bronze into the Iron ages (~2500-500 BCE). Palynology 38 (2), 280–302.
Langgut, D., Finkelstein, I., Litt, T., Neumann, F.H., Stein, M., 2015a. Vegetation and climate changes during the Bronze and Iron Ages (~3600-600 BCE) in the southern Levant based on palynological records. Radiocarbon 57 (2), 217–235.
Langgut, D., Yannai, E., Taxel, I., Agnon, A., Marco, S., 2015b. Resolving a historical earthquake date at Tel Yavneh (central Israel) using pollen seasonality. Palynology. http://dx.doi.org/10.1080/01916122.2015.1035405.
Leroy, S.A.G., 2010. Pollen analysis of core DS7-1SC (Dead Sea) showing intertwined effects of climatic change and human activities in the Late Holocene. J. Archaeol. Sci. 37, 306–316.
Leroy, S.A.G., Marco, S., Bookman, R., Miller, C.S., 2010. Impact of earthquakes on agriculture during Roman-Byzantine period from pollen records of the Dead Sea laminated sediment. Quat. Res. 73 (2), 191–200.
Litt, T., Ohlwein, C., Neumann, F.H., Hense, A., Stein, M., 2012. Holocene climate variability in the Levant from the Dead Sea pollen record. Quat. Sci. Rev. 49, 95–105.
López-Merino, L., Silva Sánchez, N., Kaal, J., López-Sáez, J.A., Martínez Cortizas, A., 2012. Post-disturbance vegetation dynamics during the late Pleistocene and the Holocene: an example from NW Iberia. Glob. Planet Change 92–93, 58–70.
Migowski, C., Agnon, A., Bookman, R., Negendank, J.F.W., Stein, M., 2004. Recurrence pattern of Holocene earthquakes along the Dead Sea transform revealed by varve-counting and radiocarbon dating of lacustrine sediments. Earth Planet. Sci. Lett. 222 (1), 301–314.
Migowski, C., Stein, M., Prasad, S., Negendank, J.F.W., Agnon, A., 2006. Holocene climate variability and cultural evolution in the Near East from the Dead Sea sedimentary record. Quat. Res. 66 (3), 421–431.
Neev, D., Emery, K.O., 1967. The Dead Sea. Depositional processes and environments of evaporates. Geological Survey of Israel, Bulletin No. 41, pp. 1–147.
Nehorai, R., Lensky, I.M., Hochman, L., Gertman, I., Brenner, S., Muskin, A., Lensky, N.G., 2013. Satellite observations of turbidity in the Dead Sea. J. Geophys. Res. Oceans 118 (6), 3146–3160.
Neugebauer, I., Brauer, A., Schwab, M.J., Dulski, P., Frank, U., Hadzhiivanova, E., Kitagawa, H., Litt, T., Schiebel, V., Taha, N., Waldmann, N., 2015. Evidences for centennial dry periods at ~3300 and ~2800 cal. yr BP from micro-facies analyses of the Dead Sea sediments. Holocene 25 (8), 1358–1371.
Neumann, F.H., Kagan, E.J., Schwab, M.J., Stein, M., 2007. Palynology, sedimentology and palaeoecology of the late Holocene Dead Sea. Quat. Sci. Rev. 26, 1476–1498.
Neumann, F.H., Kagan, E.J., Stein, M., Agnon, A., 2009. Assessment of the effect of earthquake activity on regional vegetation – high-resolution pollen study of the Ein Feshka section, Holocene Dead Sea. Rev. Palaeobot. Palynol. 155 (1–2), 42–51.
Neumann, F.H., Kagan, E.J., Leroy, S.A.G., Baruch, U., 2010. Vegetation history and climate fluctuations on a transect along the Dead Sea west shore and their impact on past societies over the last 3500 years. J. Arid Environ. 74 (7), 756–764.
Niemi, T.M., Ben-Avraham, Z., 1997. Active Tectonics in the Dead Sea Basin. In: Niemi, T.M., Ben-Avraham, Z., Gat, J. (Eds.), The Dead Sea: The Lake and its Settings. Oxford University Press, New York, pp. 73–81.
Offer, Z.Y., Zangwill, A., Azmon, E., 1992. Characterization of airborne dust in the Sde Boker area. Isr. J. Earth Sci. 41, 235–245.
Ojala, A., Alenius, T., 2005. 10 000 years of interannual sedimentation recorded in the Lake Nautajärvi (Finland) clastic-organic varves. Palaeogeogr. Palaeoclimatol. Palaeoecol. 219, 285–302.
Prasad, S., Vos, H., Waldmann, N., Goldstein, S., Stein, M., 2004. Evidence from Lake Lisan of solar influence on decadal- to centennial-scale climate variability during marine oxygen isotope stage 2. Geology 32, 581–584.

Reille, M., 1992. Pollen et Spores d'Europe et d'Afrique du Nord. Laboratoire de Botanique Historique et Palynologie, CNRS, Marseille.
Reille, M., 1995. Pollen et spores d'Europe et d'Afrique du Nord. Supplément 1. Laboratoire de Botanique Historique et Palynologie, Marseille.
Reille, M., 1998. Pollen et spores d'Europe et d'Afrique du Nord. Supplément 2. Laboratoire de Botanique Historique et Palynologie, Marseille.
Salmaso, N., Decet, F., 1998. Interactions of physical, chemical and biological processes affecting the seasonality of mineral composition and nutrient cycling in the water column of a deep subalpine lake (Lake Garda, Northern Italy). Arch. für Hydrobiol. 142, 385–414.
Shmida, A., Darom, D., 2000. Handbook of Wildflowers of Israel. Desert flora. Keter Publishing House Ltd, Jerusalem.
Shmida, A., Darom, D., 2002. Handbook of Wildflowers of Israel. Mediterranean Flora. Keter Publishing House Ltd, Jerusalem.
Singer, A., Ganor, E., Dultz, S., Fischer, W., 2003. Dust deposition over the Dead Sea. J. Arid Environ. 53, 41–59.
Stahr, K., Hermann, L., Jahn, R., 1994. Long distance dust transport in the Sudano-Sahelian Zone and the consequences for soil properties. In: Buerkert, B., Allison, B.E., Von Oppen, M. (Eds.), Wind Erosion in West Africa: the Problem and its Control. University of Hohenheim, Germany, Weikersheim, Germany, pp. 23–33. Margraf Verlag.
Stein, M., 2014. The evolution of Neogene-Quaternary water-bodies in the Dead Sea rift valley. In: Garfunkel, Z., Ben-Avraham, Z., Kagan, E. (Eds.), Dead Sea Transform Fault System: Reviews. Springer, Netherlands, pp. 279–316.
Stein, M., Goldstein, S.L., 2006. U-Th and radiocarbon chronologies of late Quaternary lacustrine records of the Dead Sea basin: methods and applications. Geol. Soc. Am. Special Pap. 401, 141–154.
Stein, M., Starinsky, A., Katz, A., Goldstein, S.L., Machlus, M., Schramm, A., 1997. Strontium isotopic, chemical, and sedimentological evidence for the evolution of Lake Lisan and the Dead Sea. Geochimica Cosmochimica Acta 61 (18), 3975–3992.
Stockmarr, J., 1971. Tablets with spores used in absolute pollen analysis. Pollen Spores 13, 614–621.
Thompson, J.B., Schultze-Lam, S., Beveridge, T.J., Des Marais, D.J., 1997. Whiting events: biogenic origin due to photosynthetic activity of cyanobacterial picoplankton. Limnol. Oceanogr. 42 (1), 133–141.
Torfstein, A., Goldstein, S.L., Kagan, E.J., Stein, M., 2013. Integrated multi-site U-Th chronology of the last glacial Lake Lisan. Geochimica Cosmochimica Acta 104, 210–231.
Waisel, Y., unpublished report 1. Survey of allergenic pollen and spores in the Kalya region 2002-2003. Tel Aviv University.
Waisel, Y., unpublished report 2. Survey of allergenic airborne pollen and spores in the Dead Sea region 1999-2002. Tel Aviv University.
Zolitschka, B., Francus, P., Ojala, A.E.K., Schimmelmann, A., 2015. Varves in lake sediments – a review. Quat. Sci. Rev. 117, 1–41.